Marine Environmental Research 216 (2026) 107897

Contents lists available at ScienceDirect

Marine Environmental Research

journal homepage: www.elsevier.com/locate/marenvrev

Sedimentary organic carbon and nitrogen storage in a recovered saltmarsh: Rewilding as a nature-based solution for anthropogenically desiccated wetlands

S. Haro [a,*], A. Corzo [b,c], S. Papaspyrou [b,c], E. García-Robledo [b,c], I. Caballero [a], G.M. Arroyo [b,c]

[a] Department of Ecology and Coastal Management, Institute of Marine Sciences of Andalusia (ICMAN), Spanish National Research Council (CSIC), 11510, Cadiz, Spain
[b] Department of Biology, Faculty of Marine and Environmental Sciences, University of Cadiz, 11510, Cadiz, Spain
[c] University Institute of Marine Research (INMAR), Puerto Real Campus, 11510, Cadiz, Spain

ARTICLE INFO

Keywords:
Rewilding
Saltmarsh
Stocks
Blue carbon
Water quality improvement
Remote sensing

ABSTRACT

Saltmarshes provide key ecosystem services, including atmospheric CO_2 sequestration and nitrogen burial in sediments. In recent decades, these blue carbon ecosystems have faced significant degradation from natural and anthropogenic stressors. In this study, rewilding of a desiccated saltmarsh in Cadiz Bay (SW Spain) was assessed as a nature-based solution to restore carbon (C_{org}) and nitrogen (N_T) storage. The rewilding process began in 2004 after breaching an external tidal wall. We evaluated changes in vegetated and unvegetated areas using Landsat satellite imagery (1994–2024) and quantified C_{org} and N_T stocks and burial rates in wild and rewilded sediments, including vegetated saltmarsh (*Sarcocornia* sp.) and bare sediments colonized by microphytobenthos (MPB). Vegetated saltmarsh cover increased by 85% over 20 years, at an average recovery rate of 5 ha y^{-1}, concurrent with a decrease in unvegetated tidal flats. Average C_{org} stocks in the top 1 m ranged from 32 to 57 t C_{org} ha^{-1}, with higher values in vegetated sediments. However, only 5–12% of C_{org} was stored during the rewilding period. C_{org} burial rates averaged 69 g C_{org} m^{-2} y^{-1}, and N_T stocks were 55% higher in rewilded sediments than in wild ones (3.6 vs. 1.6 t N_T ha^{-1}). Despite vegetation recovery, burial rates of C_{org} and N_T did not increase clearly, suggesting that long-term storage may be influenced by factors beyond rewilding. Less than 8% of sedimentary C_{org} originated from saltmarsh vegetation, indicating the dominance of allochthonous sources. These findings highlight the complexity of biogeochemical recovery in rewilded saltmarshes and underscore the need for long-term monitoring to determine how much time is truly required for C_{org} and N_T recovery.

1. Introduction

Saltmarshes are dynamic coastal environments, providing a wide range of essential ecosystem services, including coastal protection, carbon sequestration, nutrient cycling, biodiversity support, and opportunities for recreation and sustainable livelihoods (Barbier et al., 2011; Martin et al., 2020). Among these, their role as blue carbon reservoirs, as well as their capacity to retain and process other nutrients such as nitrogen, is particularly significant for mitigating climate change and eutrophication (Duarte et al., 2005; Howard et al., 2017). Blue carbon refers to the organic carbon (C_{org}) captured and stored by coastal ecosystems, such as wetlands (i.e., saltmarshes, mangroves, and intertidal seagrass meadows) or subtidal ecosystems (Macreadie et al., 2019; McLeod et al., 2011), and is usually quantified as the C_{org} stored within the first meter of marine sediments over the long term (Howard et al., 2014). Photosynthetic organisms fix atmospheric CO_2, which is incorporated into plant debris and detritus that accumulates in the sediment. Low-oxygen conditions slow OM decomposition, allowing C_{org} to build up and become buried over time, including both locally produced (autochthonous) and externally derived OM (allochthonous) (Duarte et al., 2005; Middelburg et al., 1997). Among these ecosystems, saltmarshes are the second most effective in carbon sequestration and storage, despite covering less than 2% of the global ocean area (Murray et al., 2019). They are estimated to store up to 400 t C_{org} ha^{-1} in their sediments over the long term, equivalent to approximately 1467 t CO_2 ha^{-1}, highlighting their importance as a significant carbon sink within

* Corresponding author.
E-mail address: sara.haro@csic.es (S. Haro).

https://doi.org/10.1016/j.marenvres.2026.107897
Received 22 October 2025; Received in revised form 22 January 2026; Accepted 29 January 2026
Available online 31 January 2026

coastal ecosystems (Mason et al., 2023; Temmink et al., 2022).

In addition to C_{org} sequestration, saltmarshes play a crucial role in many biogeochemical processes, particularly in the removal of total nitrogen (N_T) from the water column and its retention in sediments. N biogeochemical cycling is complex and occurs in sediments through multiple microbial pathways in oxic and anoxic conditions. Under anoxic conditions, a fraction of C_{org} is mineralised through denitrification, a process that converts dissolved inorganic nitrogen, mainly nitrate (NO_3^-), into dinitrogen gas (N_2), which is subsequently released to the atmosphere (Moseman-Valtierra et al., 2011; Yang et al., 2022). Denitrification alleviates eutrophication by removing reactive nitrogen from the water column, but it can also contribute to the greenhouse effect due to the release of nitrous oxide (N_2O) as a by-product (Burden et al., 2013). However, a significant fraction of nitrogen may also be retained in sediments via OM burial or adsorption onto sediment particles. Overall, recent estimates indicate that saltmarsh sediments, in addition to C_{org}, retain N_T, as both variables are frequently correlated. Nevertheless, few studies have examined N_T density profiles or quantified the N_T reservoir in tidal sediments (Casal-Porras et al., 2022; Martins et al., 2022; Santos et al., 2019).

Despite their crucial role in sequestration C_{org} and retaining N_T in sediments, saltmarshes are under significant threat from human activities, with global losses of saltmarsh areas estimated between 25% and 50% since the early 20th century (Burden et al., 2013; Duarte et al., 2005; Pendleton et al., 2012). Larger losses are also expected due to climate change-driven processes, including sea-level rise and increased storm frequency and intensity (Saintilan et al., 2022). Saltmarshes have been extensively degraded due to land reclamation for agriculture, aquaculture, salt production, port development, and other uses, frequently leading to the alteration of their hydrological regimes and desiccation. Saltmarsh desiccation alters the biogeochemical conditions of the sediment, shifting natural anaerobic conditions to aerobic (Gore et al., 2024). This change facilitates the remineralization of C_{org} stored within sediments, resulting in CO_2 release into the water and/or air, as well as substantial losses of ecosystem functions and services. Moreover, anthropogenic nutrient inputs from agriculture, livestock farming, and other activities have intensified eutrophication in these altered systems as well (Lotze et al., 2006; Mei et al., 2025; Pendleton et al., 2012).

Effective recovery and conservation of ecosystem services and functions depend on mitigating anthropogenic pressures and restoring the natural role of degraded habitats (Adams et al., 2021; Pétillon et al., 2023). Ecological restoration aims to assist the recovery of a damaged or degraded ecosystem toward a specified reference condition, by means of active human interventions to accelerate or enhance the process (McDonald et al., 2016; Perino et al., 2019). In contrast, rewilding has emerged more recently as an alternative and complementary nature-based approach, in which the main focus is not to recreate a previous target ecological community or function, but to allow the development of a well-functioning and resilient ecosystem governed by natural processes rather than human management (Pettorelli and Bullock, 2023). Rewilding can occur without human intervention or be initiated by minimal interventions that remove anthropogenic constraints, after which ecosystem recovery proceeds primarily through natural processes; this pathway is also referred to as natural regeneration or passive restoration (Gann et al., 2019). Within its regulatory framework, the European Union (EU) has recently approved the Nature Restoration Law (EU Regulation, 2024/1991) to restore at least 20% of the EU's degraded coastal ecosystems, including saltmarshes, by 2030 and to promote their long-term resilience.

These conceptual and regulatory developments have coincided with a growing scientific interest in saltmarsh recovery, as evidenced by the exponential increase in studies over the last 20 years. So far, most saltmarsh recovery studies have been done in the United States (58%), followed by Europe (35%), particularly in the UK (9%), with important contributions from Australia and China in recent years (Mason et al., 2023). Most of these studies investigated active human interventions of different intensities (e.g., species reintroduction, habitat modification, or environmental management actions) on degraded saltmarshes (82%), whereas only about 18% addressed passive approaches (Gonçalves et al., 2024). The elimination of physical barriers to tidal flow in desiccated saltmarshes, which can occur naturally (e.g., storm-induced breaches) or through minimal, one-time human intervention, represents a rewilding approach that helps restore natural hydrological regimes and sediment dynamics and promotes the growth of saltmarsh vegetation. Tidal restoration has been shown to enhance key ecosystem services, such as the sequestration of C_{org} and the retention of N_T in sediments, contributing to nutrient regulation in coastal systems (Beers et al., 2020; Stewart-Sinclair et al., 2024). Sedimentary C_{org} and N_T dynamics are shaped by tidal regime, vegetation zonation, sedimentation rates, and microbial biogeochemical cycling, which influence OM mineralization, nutrient transformation, and long-term storage (Barry et al., 2022; de los Santos et al., 2023; Jiménez-Arias et al., 2020). Further research is needed to investigate how re-establishment of natural hydrological regimes affects saltmarsh recovery, sediment biogeochemistry and ecosystem functioning. Freely available multispectral satellite imagery, such as the Landsat series (30 m spatial resolution, operational since the late 1980s) and Sentinel-2 (10 m, since 2015), provide an effective tool to monitor spatiotemporal changes in intertidal photosynthetic communities and assess the outcomes of restoration or rewilding processes (Curcio et al., 2023; Haro et al., 2022; Lopes et al., 2019; Naojee et al., 2024).

Here, we analyse rewilding as a nature-based solution for a desiccated saltmarsh in a tidal channel within the Cadiz Bay Natural Park, southwest Spain (Fig. 1). The specific objectives are: 1) to evaluate spatiotemporal changes in bare sediment communities (unvegetated sediment) and the higher plant saltmarsh vegetation (vegetated sediment) after the breach of the tidal wall in 2004, using Landsat imagery, in comparison with a nearby reference saltmarsh, from 1994 to 2024; 2) to quantify and compare C_{org} and N_T storage in the unvegetated and vegetated sediments of reference and rewilded saltmarshes at depths of up to 100 cm, with particular attention to the C_{org} and N_T buried and stored after two decades of rewilding; and 3) to investigate the possible differences in the origin of C_{org}, through $\delta^{13}C$ isotopic analysis, accumulated in both vegetated and unvegetated sediments of both the reference saltmarsh and the saltmarsh undergoing the rewilding process. This research highlights the role of saltmarsh rewilding in enhancing the storage of C_{org} and N_T, and in restoring ecosystem services that support climate regulation and help control eutrophication.

2. Methodology

2.1. Study area

C_{org} and N_T storage in sediments were quantified in a reference mature saltmarsh located in 'Los Toruños' Metropolitan Park (hereafter referred to as wild saltmarsh, 36° 34′ 33.07″ N, 6° 12′ 40.57″ W) and in a saltmarsh undergoing a rewilding process in the Rio de San Pedro tidal channel (hereafter referred to as rewilded saltmarsh, 36° 33′49.65″ N, 6° 11′ 46.61″ W), both located within the boundaries of Cadiz Bay Natural Park, SW Spain (Fig. 1). Cadiz Bay has tidal ranges of approximately 2–4 m (neap and spring tides, respectively) and a moderate wave climate that propagates mainly from the Atlantic Ocean with a limited incursion inside the bay (González et al., 2023; Zarzuelo et al., 2023). The rewilded saltmarsh was desiccated in 1958 for its transformation to agricultural land through the construction of an embankment or tidal wall that restricted tidal flow (Fig. S1) (Gracia et al., 2017). However, due to the high salinity of the soils, cultivation was not feasible, and the tidal wall was partially opened in 2004. This minimal, one-time human intervention, consisting of the breaching of the tidal wall, removed an anthropogenic barrier and reinstated natural tidal dynamics, leading to a progressive natural recovery of the saltmarsh and initiating the rewilding process without further management actions (de Lomas et al.,

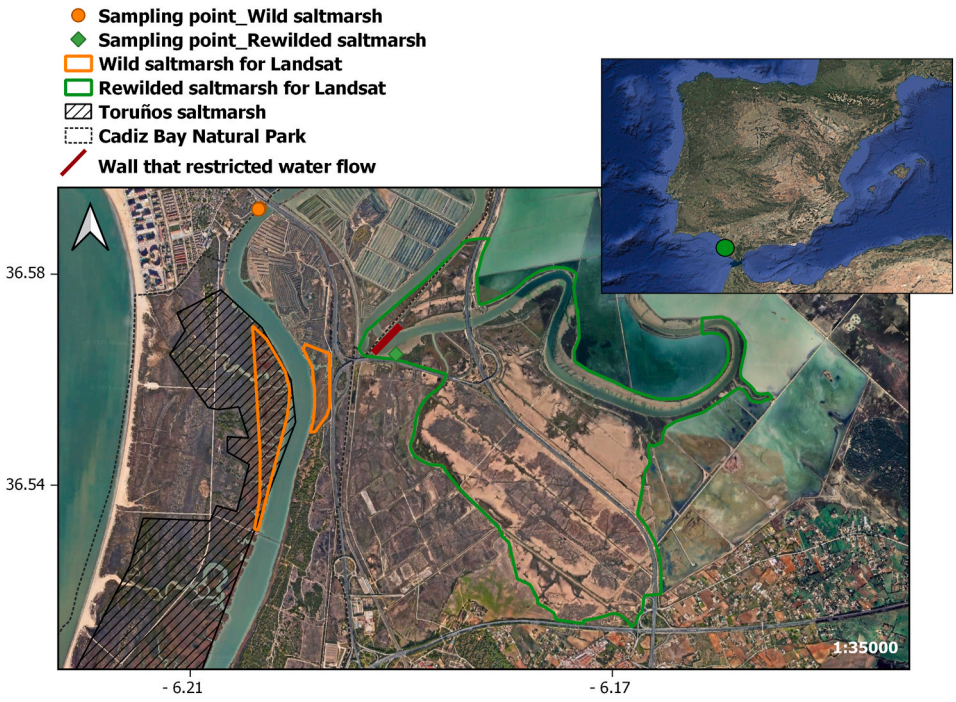

Fig. 1. Sampling points in a wild saltmarsh (orange point) and a rewilded saltmarsh (green point) at the boundary of the Cadiz Bay Natural Park, where nutrient storage was quantified. Saltmarsh rewilding (green polygon) in the Rio San Pedro tidal channel (Cadiz Bay, SW Spain) began in 2004 with an intervention involving the opening of the external tidal wall (indicated in red). The wild saltmarsh (orange polygon) was used as a control for comparison with the rewilded site. Both sites were also monitored using Landsat imagery. (For interpretation of the references to colour in this figure legend, the reader is referred to the Web version of this article.)

2008). To study the effects of the rewilding process on saltmarsh vegetation, 588.9 ha of rewilded saltmarsh was assessed using Landsat series imagery. In addition, a nearby area of 45.5 ha of wild saltmarsh was selected exclusively as a reference area to demonstrate that the temporal changes observed in saltmarsh vegetation in the rewilded saltmarsh are unlikely to be driven solely by regional or natural variability. This reference area was not used to estimate vegetation recovery rates or to scale biogeochemical rates, thereby avoiding potential biases related to differences in saltmarsh size. In general, the Cadiz Bay Natural Park coastal system consists of saltmarshes, characterized by low-to mid--marsh zones dominated by *Sporobolus maritimus* and *Sarcocornia* sp., respectively, and adjacent tidal flats, which are bare sediments mainly covered by benthic microalgae (microphytobenthos, MPB) (Curcio et al., 2023).

2.2. Monitoring saltmarsh vegetation recovery using landsat series imagery

Landsat series satellite imagery from the Landsat-5 and Landsat-8 missions was used to monitor saltmarsh vegetation recovery between 1994 and 2024 (10 years before and 20 years after the opening of the wall). The study area was delineated using a manually predefined polygon representing the extent of the saltmarsh under recovery (i.e., undergoing rewilding), traced from Google Earth (shapefile; green line; Fig. 1). Landsat images were manually selected for each summer (one per year; Table S1), ensuring acquisition during low tide and under cloud-free conditions. Image visualizations (True Colour and False Colour composites) were performed through the Copernicus Data Space Ecosystem (https://browser.dataspace.copernicus.eu). True-colour composites were generated by combining the red, green, and blue bands (Bands 3-2-1 for Landsat 5 TM and Bands 4-3-2 for Landsat 8 OLI) and False-colour composites were created using near-infrared, red, and green bands (Bands 4-3-2 for Landsat 5 TM and Bands 5-4-3 for Landsat 8 OLI). Subsequently, the preselected images were processed by means of the Google Earth Engine (GEE) platform (Earth Engine Code Editor; https://code.earthengine.google.com/). Two imagery collections (Collection 2; Tier 1; Level 2) were utilized: Landsat-5, covering the period from 1994 to 2012, and Landsat-8, from 2013 to 2024.

The GEE workflow was structured as follows. Surface reflectance values of the optical bands were adjusted using a scaling factor in accordance with Landsat specifications (https://www.usgs.gov/landsat-missions/landsat-collection-2-level-2-science-products). Reflectance bands were scaled using the equation: Scaled value = Original value × 0.0000275 − 0.2. Subsequently, the Normalized Difference Vegetation Index (NDVI) was calculated for each image using reflectance from the near-infrared (NIR; Band 4 for Landsat-5 and Band 5 for Landsat-8) and red bands (Band 3 for Landsat-5 and Band 4 for Landsat-8), following the equation NDVI = (NIR − Red)/(NIR + Red). A threshold of NDVI $\geq$0.25 was applied to isolate areas covered by saltmarsh vegetation, while bare sediment, with or without MPB, was classified with NDVI values between 0 and 0.249. In inner Cadiz Bay, NDVI threshold of 0.3 have been used previously to isolate saltmarsh vegetation (Curcio et al., 2023), while maximum NDVI values for MPB remain below 0.35 (Haro et al., 2022), resulting in only a slight potential overlap. However, as MPB has been shown to reach higher biomass (i.e., NDVI values) during winter in temperate southern European tidal systems (e.g., the inner Cadiz Bay), and all analysed images were acquired during summer, this overlap is effectively negligible. Thus, the selected threshold of 0.25 is conservative and reliably distinguishes saltmarsh vegetation from MPB. Water was identified using the Normalized Difference Water Index (NDWI) with values > 0. Each NDVI raster was then clipped to the predefined study area polygon to focus on the target ecosystem, and the processed rasters were exported to Google Drive as GeoTIFF files with a spatial resolution of 30 m, using the UTM Zone 29N coordinate reference system (EPSG:32629).

Once the NDVI rasters were downloaded, they were mapped and analysed using QGIS software (version 3.10, 'A Coruña'). Annual variability for each category (saltmarsh vegetation, bare sediment with

MPB, and water) was assessed using the 'Zonal Statistics' tool. Two key metrics were evaluated: cover, represented by the number of pixels classified within each category, and average NDVI, calculated for the entire area of the recovering saltmarsh (Haro et al., 2022). These metrics provided quantitative insights into benthic photosynthetic biomass (saltmarsh vegetation or MPB) and the annual recovery rates of the vegetated rewilded saltmarsh (Fig. S2).

2.3. Sediment characterization and biogeochemical profiles

Twelve sediment cores (internal diameter = 6 cm; length = 100 cm) were sampled in May 2021 from wild and rewilding saltmarshes. In each saltmarsh, three cores were collected from unvegetated sediments, primarily covered by MPB, and three from vegetated sediments, predominantly consisting of *Sarcocornia* spp., whose aboveground biomass was manually removed without disturbing the sediment. Sediment cores were collected, transported immediately to the laboratory and frozen until further processing.

In the laboratory, sediment cores were cut longitudinally with an electrical saw (avoiding PVC particles from falling onto the sediment) and then sediment slices were sectioned at 2 cm intervals. The sediment samples were subsequently lyophilized. The sediment cores were analysed following the procedure proposed in the blue carbon manuals (Howard et al., 2014). Profiles of sediment dry bulk density (DBD), organic matter (OM), organic carbon (C_{org}), and C_{org} density were analysed. In addition, profiles of inorganic carbon (C_{in}), total nitrogen (N_T) and $\delta^{13}C$ isotopic analysis in the sediments were measured. DBD was determined as the dry sediment weight divided by the initial volume. The OM was measured by loss on ignition (Heiri et al., 2001). Total carbon (C_T) and N_T contents were determined in dried sediment samples. C_{org} was determined as the difference between C_T measured in dried sediment samples and C_{in} measured on a second replicate combusted previously at 550 °C for 5 h. Both samples were analysed on an Elemental Analyzer Flash EA112 (Thermos Finnigan) at the Central Services of the University of A Coruña. DBD and OM were measured in all 2-cm slices, whereas elemental C and N were analysed only in slices at 2, 4, 6, 8, 10, 14, 18, 22, 26, 30, 40, 50, 60, 70, 80, and 90 cm (uncorrected for compaction).

Sediment compaction was assumed to be linear and was estimated by recording the difference in length from the top of corer to the sediment surface, inside and outside the core liner, after insertion into the sediment (Howard et al., 2014). The core compaction (average ± standard deviation) was 35 ± 22% for unvegetated and 60 ± 14% for vegetated sediments in the rewilding saltmarsh, while in the wild saltmarsh, the compaction percentages were 26 ± 10% for unvegetated and 0 ± 17% for vegetated sediments. After applying the respective compaction factors, 2-cm slice data were averaged into corrected 5-cm depth intervals (0–5, 5–10, 10–15, 15–20, 20–25, 25–30, 30–40, 40–50, 50–60, 60–70, 70–80, 80–90, and 90–100 cm) to avoid mixing slices from different depths.

2.4. Storage and burial rates of organic carbon and total nitrogen

Densities of C_{org} and N_T were calculated from DBD and their % content and expressed in both g cm^{-3} and g cm^{-2}, after applying compaction factors and assigning corrected depth intervals. Due to substrate hardness, sediment cores were collected to depths ranging from 60 to 90 cm. C_{org} and N_T stocks were quantified (summed) from the vertical profiles of C_{org} density (t C_{org} ha^{-1}) and N_T density (t N_T ha^{-1}), respectively, and estimated up to a depth of 1 m ($C_{org\text{-}100cm}$ stock; $N_{T\text{-}100cm}$ stock), assuming that C_{org} and N_T densities remained constant in the deeper sediment layers. This approach facilities comparison with values reported in the literature. C_{org} stocks in wild and rewilding saltmarsh sediments were also converted to CO_2 equivalents (t CO_2 ha^{-1}).

To assess the effects of rewilding on the storage and burial rates of C_{org} and N_T, we assumed a sediment accretion rate (SAR) of 0.69 ± 0.38 cm y^{-1}, corresponding to recent average SAR values averaged over 100 years (SAR_{100y}) reported for vegetated mid-saltmarshes dominated by *Sarcocornia* sp. in the saltmarshes of 'Los Toruños' and 'Odiel', both located in the western coastal region of southern Spain (Andalusia) (Díaz-Almela et al., 2019, 2021). Based on the uncertainty (standard deviation) associated with this regional SAR, the upper 12 cm of sediment were estimated to represent the last 17 years before sampling (from 2021 to 2004), with a plausible depth range of 5–18 cm when this uncertainty is considered. This range reflects reported SAR variability along the sediment column (0.31–1.07 cm y^{-1}) over centennial timescales in these mid-vegetated saltmarshes. Therefore, the upper ~20 cm of sediment were assumed to have accumulated conservatively during the 20-year rewilding process. Based on these assumptions, C_{org} and N_T storage were quantified for the upper 20 cm of sediment ($C_{org\text{-}20cm}$ stock; $N_{T\text{-}20cm}$ stock), and average burial rates of C_{org} and N_T during the rewilding process, expressed as g C_{org} m^{-2} y^{-1} and g N_T m^{-2} y^{-1}, were estimated as a first-order approximation for both vegetated and unvegetated sediments in the wild and rewilded saltmarsh.

2.5. Organic carbon isotopic analysis and Bayesian mixing model

Sediment homogenized samples for $\delta^{13}C$ analyses were acidified with 2 N HCl to remove C_{in} (Komada et al., 2008). $\delta^{13}C$ isotopic samples were analysed on a Flash IRMS coupled via a Conflo IV interface to a Delta V Advantage isotope ratio mass spectrometer (ThermoScientific) (Central Services of the University of A Coruña). Stable isotope mole fractions of C_{org} are given in delta notation (‰) relative to Vienna PeeDee Belemnite (VPDB) and atmospheric air, respectively. Due to the high cost of isotopic analysis, only one core per typology was isotopically measured. In addition, note that $\delta^{13}C$ measurements were taken at the same depths as C_{org} and N_T.

Bivariate boxplot of the elemental and isotopic composition (i.e., $\delta^{13}C$ versus C_{org}:N_T ratio) for studied saltmarsh sediments were plotted using the 'ggplot2', 'MASS', and 'ggforce' packages in RStudio (version 2022.07.2) (Pedersen, 2016; Venables and Ripley, 2022; Wickham, 2016). Visual examination of the bivariate data was conducted using the bag-plot, where the ellipses representing the central 50 % of the data (bags) and the outliers were calculated and visualized using the stat_ellipse function from the 'ggforce' package. The contributions of the various potential sources to the sediment OM were determined using a Bayesian stable isotope mixing model implemented with the 'simmr' package (Parnell et al., 2013). This model was applied from a dataset of $\delta^{13}C$ values and C_{org}:N_T ratios compiled by Jiménez-Arias et al. (2020), which included potential OM sources (e.g., green, brown and red seaweeds, seagrass, saltmarsh vegetation and suspended particulate material) for the intertidal sediments of Cadiz Bay. These values were consistent with those later measured by de los Santos et al. (2023) for most macrophytes in the area. Unfortunately, the isotopic composition of MPB remains largely understudied worldwide, with existing datasets sparse and poorly constrained (Herman et al., 2000; Middelburg et al., 2000), and consequently, it was excluded from the Bayesian stable isotope mixing model.

2.6. Statistical analysis

Generalized linear mixed models (GLMMs) with a Gamma distribution and log-link function were used to evaluate the effects of saltmarsh type (wild vs. rewilded), sediment subtype (vegetated vs. unvegetated), and sediment depth (5, 10, 15, 20, 25, 30, 40, 50, 60, 70, 80 and 90 cm) on DBD, %OM, %OC, %Cin, $\%N_T$, and densities of C_{org} and N_T (g cm^{-3}). Core was included as a random effect to account for differences in core length. Interactions between saltmarsh type and subtype were assessed using post-hoc pairwise comparisons with Tukey adjustment (Equation (1)). For all models, wild saltmarsh, unvegetated sediments, and the 0 cm depth interval were set as the reference categories for interpreting fixed effects, which were evaluated based on model coefficients and

their associated p-values. All statistical analyses were conducted in RStudio (version 2022.07.2) using the packages 'lme4', 'emmeans' and 'readxl' (Bates et al., 2015; Lenth and Piaskowski, 2025; Wickham and Bryan, 2015).

$$C_{org}\ density \sim SaltmarshType * SaltmarshSubtype + DepthIntervals + (1 \mid Core) \quad \text{(Equation 1)}$$

Stocks of C_{org} and N_T (t ha^{-1}) in the top 20 cm of sediment ($C_{org\text{-}20cm}$ stock; $N_{T\text{-}20cm}$ stock), as well as in the upper 100 cm ($C_{org\text{-}100cm}$ stock; $N_{T\text{-}100cm}$ stock), were analysed using two-way ANOVAs with factors saltmarsh type and sediment subtype. Log transformations were applied when data did not meet the assumption of normality (Shapiro-Wilk test). After the two-way ANOVAs, post-hoc comparisons with Tukey's Honest Significant Difference (HSD) test were performed to evaluate differences between saltmarsh type (wild vs. rewilded) and subtype (vegetated vs. unvegetated) for stocks at 20 cm (representing nutrients potentially stored during rewilding) and at 100 cm (i.e., blue carbon). Two-way ANOVAs and post-hoc HSD comparisons were also used for the burial rates of C_{org} and N_T in the upper 20 cm of sediment. All statistical analyses were conducted in RStudio (version 2022.07.2) using the 'stats', 'car', 'multcomp', 'multcompView', and 'readxl' packages (Fox and Weisberg, 2011; Graves et al., 2012; Hothorn et al., 2008). All results are interpreted in the view of statistical clarity following the recommendations of Dushoff et al. (2019).

3. Results

3.1. Monitoring saltmarsh rewilding using remote sensing

The extent of the rewilded saltmarsh undergoing the rewilding process covered a total area of 588.9 ha (Fig. 1). Water cover ranged between 18.5 and 57.1 ha throughout the study period (i.e., less than 10% of the total area) (Fig. 2; Fig. 3a). Before the rewilding process began in 2004 (Fig. S1), saltmarsh vegetation cover was very low (~34 ha in 2003, ca. 5.7%). Most of the area consisted of bare, unvegetated sediment, which accounted for 91% of the desiccated saltmarsh, with an

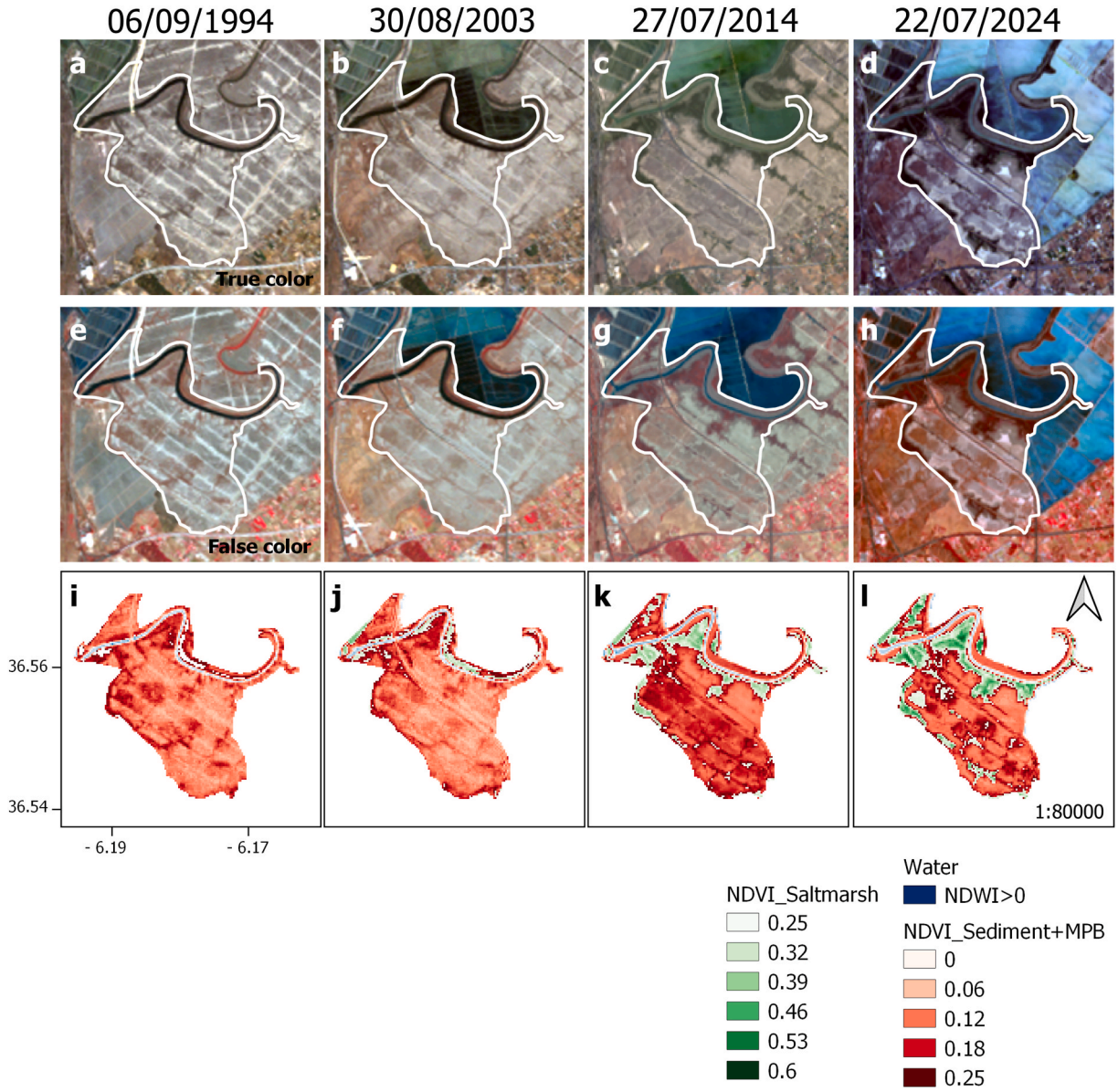

Fig. 2. Saltmarsh extent before and after the rewilding process initiated in 2004, showing ten years before (1994), one year before (2003), ten years after (2014), and twenty years after (2024), based on Landsat multispectral imagery. The figure includes *True-color* and False-color compositions, as well as classified maps based on NDVI analysis. Scale 1:80,000. (For interpretation of the references to colour in this figure legend, the reader is referred to the Web version of this article.)

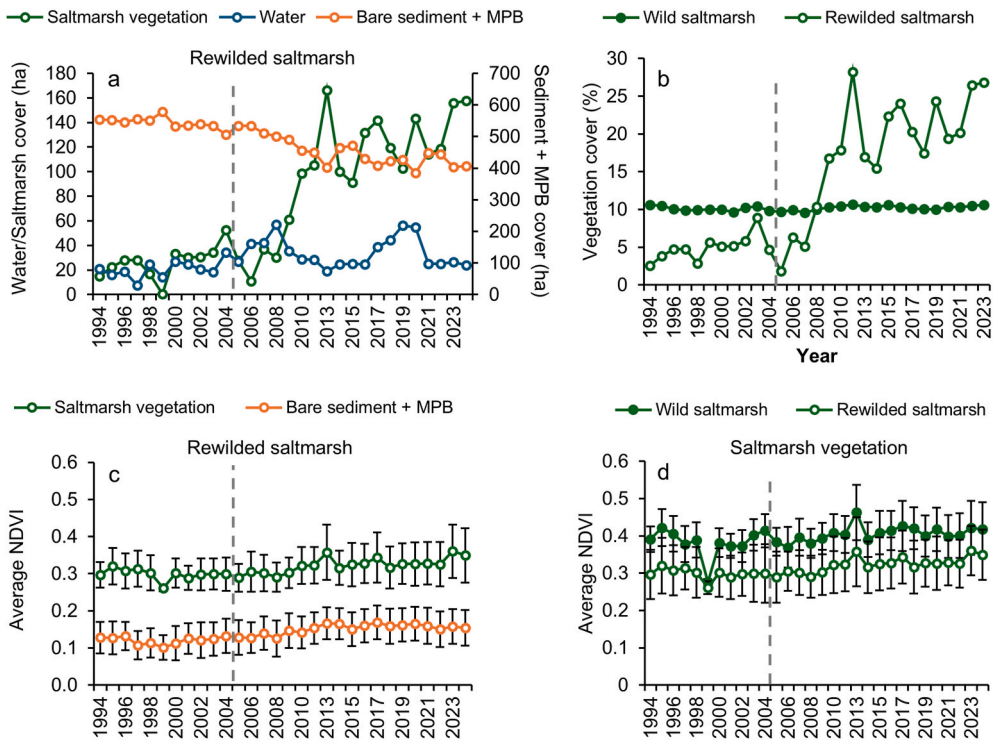

Fig. 3. Annual changes in: (a) cover (ha and %) of water, saltmarsh vegetation, and bare sediment with/without microphytobenthos (MPB) in the rewilded saltmarsh; (b) saltmarsh vegetation cover (%) in wild and rewilded saltmarshes; (c) mean NDVI for saltmarsh vegetation and bare sediment with MPB in the rewilded saltmarsh; and (d) mean NDVI of saltmarsh vegetation in wild and rewilded saltmarshes. All values were derived from Landsat imagery. Rewilding began in 2004 following the removal of the wall that restricted tidal flow (grey dashed line). Data cover the period 1994–2024.

average NDVI of 0.124 ± 0.045 (Fig. 2). Saltmarsh cover reached its minimum (11 ha) two years after the tidal wall was reopened in 2004, followed by a pronounced and progressive recovery that peaked in 2013 (166 ha) with wide fluctuations in subsequent years (Fig. 3a). Saltmarsh vegetation stabilised between 2020 and 2024, reaching values of ~140 ha (23.8% of the analysed area), which reflects an 85% increase since 2004. In contrast, vegetation in the control (wild) saltmarsh remained stable during this period, consistently covering 10.2 ± 0.3% (4.7 ± 0.1 ha) of the analysed area, showing a mean NDVI of 0.42 ± 0.02 (Fig. 3c). In the rewilded site, bare sediment (whether colonised by MPB or not) showed a trend opposite to that of saltmarsh vegetation (Fig. 3a). The average NDVI of saltmarsh vegetation and bare sediment over the past 30 years were 0.314 ± 0.022 and 0.140 ± 0.004, respectively (Fig. 3c). After the opening of the wall in 2004, the MPB NDVI oscillated between 0.132 and 0.154. In contrast, NDVI for saltmarsh vegetation increased from 0.299 in 2008 to 0.349 in 2024. Although this value remains slightly lower than the average NDVI recorded for wild saltmarsh vegetation, it represents a 16.7% relative increase in NDVI for the rewilded saltmarsh vegetation (Fig. 3d).

3.2. Sediment characteristics and content in organic matter, carbon and nitrogen

In the rewilded saltmarsh, the sediment was dark grey, characteristic of fine, muddy material with a high percentage of grains smaller than 63 μm, while in the wild saltmarsh, the upper 40 cm consisted of muddy sediment as well, but a transition was observed from a sandier composition in the deeper layers (Fig. S3). The mean DBD was lower in rewilded saltmarsh compared to wild saltmarsh ($p < 0.001$, GLMM; Fig. S4a and b). In unvegetated sediments, values ranged from 0.42 to 0.61 g cm^{-3} (rewilded) and 0.62–1.36 g cm^{-3} (wild). In vegetated sediments, average DBD was also lower in the rewilded saltmarsh compared to the wild one (Table 1; $p < 0.001$, GLMM). A clear increase in DBD with depth was observed in wild sediments from 10 cm downward (all $p < 0.05$, GLMM). The GLMM results are summarized in Table 2.

OM, C_{org}, and N_T contents (%) were clearly higher in the rewilded saltmarsh than in the wild saltmarsh, and in vegetated sediments compared to unvegetated ones (Fig. S4; Fig. S5; Table 1). OM, C_{org}, and

Table 1
Averages (Av.) and standard deviation (SD) of dry bulk density (DBD, g cm^{-3}), organic matter (OM, %), organic carbon (C_{org}, %), inorganic carbon (C_{in}, %), total nitrogen (N_T, %) for a wild saltmarsh and in a rewilded saltmarsh, both in non-vegetated sediments and in vegetated sediments.

		DBD (g cm^{-3})		OM (%)		C_{org} (%)		C_{in} (%)		N_T (%)	
		Av	SD	Av	SD	Av	SD	Av	SD	Av	SD
Wild saltmarsh	**Unvegetated**	1.1	0.4	6.1	3.0	0.9	0.4	2.4	0.6	0.1	0.0
	Vegetated	1.3	0.5	7.6	4.5	1.7	0.8	1.7	0.6	0.1	0.0
	Av ± SD	1.2	0.4	6.8	3.9	1.3	0.7	2.1	0.7	0.1	0.0
Rewilded saltmarsh	**Unvegetated**	0.6	0.3	10.6	1.8	1.6	0.3	1.6	0.3	0.1	0.0
	Vegetated	0.5	0.1	11.4	2.0	2.1	0.5	1.3	0.2	0.2	0.0
	Av ± SD	0.6	0.2	11.0	2.0	1.9	0.5	1.4	0.3	0.14	0.03

Notes: N varies between 27 and 86 depending on the biogeochemical variable, sediment core length, and saltmarsh type/subtype. Statistical significance of differences is explicitly addressed using generalized linear mixed models (Table 2).

Table 2
Summary of the generalized linear mixed model (GLMM) results for sediment profiles in wild and rewilded saltmarshes, considering vegetated and unvegetated sediment layers.

Variable	Saltmarsh type (Rewilded vs Wild)	Saltmarsh subtype (Vegetated vs Unvegetated)	Depth (relative to 0 cm)	Interaction (Type × Subtype)
DBD (g cm^{-3})	↓ ***	ns	↑ 10–80 cm **	↓ Rewilded x Vegetated ***
OM (%)	↑ ***	↑ **	↓ 25–80 cm *	ns
C_{org} (%)	↑ ***	↑ **	↓ 30–80 cm *	ns
C_{org} density (g cm^{-3})	·	↑ ***	↓ 80 cm ***	↓ Rewilded x Vegetated **
N_T (%)	↑ ***	↑ *	↓ 30–80 cm *	ns
N_T density (g cm^{-3})	↑ **	↑ ***	↓ 50–80 cm *	↓ Rewilded x Vegetated *
C_T (%)	ns	ns	↓ 25–60 cm *	ns
C_{in} (%)	↓ ***	↓ **	↑ 70–80 cm *	ns

Notes: Wild saltmarsh, unvegetated sediments, and 0 cm depth are the reference categories. Arrows indicate significant increases (↑) or decreases (↓) relative to the reference. Significance codes for model estimates and post-hoc Tukey HSD comparisons: ***p < 0.001, **p < 0.01, *p < 0.05, . p ≤ 0.1 (marginal significance). ns = not significant.

N_T contents were largely associated with DBD (Fig. S6) and strongly intercorrelated (Fig. S7). These relationships varied between sites, the wild vegetated saltmarsh showing a pattern that stood out among the other environments. OM content was 54% higher in the rewilded saltmarsh (Table 1) than in the wild saltmarsh (p < 0.001, GLMM; Table 2), with a slight increase (~1%) observed in vegetated sediments (p = 0.009, GLMM). Similar patterns were found for C_{org} (Fig. S5a and b), with higher values in the rewilded than in the wild saltmarsh (Table 1; p < 0.001), and in vegetated than in unvegetated sediments (p < 0.01). N_T content also followed this trend (Fig. S5e and f), being greater in the rewilded than in the wild saltmarsh (p < 0.001), and in vegetated than in unvegetated sediments (p = 0.037). Contents of OM, C_{org} and N_T decreased clearly with depth, particularly from 25 to 30 cm downward, especially in vegetated sediments (all p < 0.05). N_T in unvegetated sediments remained relatively stable in the top 30 cm. Unlike the other variables, C_{in} content was higher in the wild saltmarsh than in the rewilded one, and in unvegetated sediments compared to vegetated ones (Fig. S5 c, d; Table 1).

3.3. Organic carbon and nitrogen stocks from density profiles

C_{org} density (g cm^{-3}) differed clearly between vegetated and unvegetated sediments (p < 0.001, GLMM, Table 2), with higher C_{org} density in vegetated (0.016 ± 0.007 g cm^{-3}) than in unvegetated wild saltmarsh sediments (0.007 ± 0.004 g cm^{-3}) (Fig. 4a and b). No clear differences were detected between wild (0.012 ± 0.007 g cm^{-3}) and rewilded saltmarsh (0.009 ± 0.003 g cm^{-3}). A clear interaction between saltmarsh type (wild vs. rewilded) and sediment subtype (vegetated vs. unvegetated) indicated that the positive effect of vegetation on C_{org} density was smaller in rewilded than in wild sediments (p < 0.001). Depth intervals showed no clear differences in the upper layers, with clear decreases observed only in deeper sediments: C_{org} density declined at 80 cm (p < 0.001), and N_T density at 50–80 cm (p ≤ 0.016).

Overall, $C_{org\text{-}100cm}$ stocks tended to be lower in wild (30.5 ± 11.0 t C_{org} ha^{-1}) than in rewilded saltmarshes (47.9 ± 11.0 t C_{org} ha^{-1}), equivalent to 111.7 and 175.7 t CO_2 ha^{-1}, respectively (Fig. 5a) (F = 10.656, p = 0.012, two-way ANOVA). In addition, $C_{org\text{-}100cm}$ was slightly higher in vegetated sediments (45.2 ± 14.1 t C_{org} ha^{-1}) than in unvegetated sediments (33.2 ± 11.9 t C_{org} ha^{-1}) (F = 4.480, p = 0.067, two-way ANOVA), although this difference was not statistically clear. Two-way ANOVA results were summarized in Table S3.

The N_T densities were highest in the upper 30 cm of wild saltmarsh sediments, decreasing gradually below that depth (Fig. 4c and d). The decrease was statistically clear in the deepest layers, especially in unvegetated sediments. Within the wild saltmarsh, N_T density was notably lower in unvegetated sediments (range 0.0001–0.0005 g N_T cm^{-3}) than in vegetated areas (range 0.001–0.0001 g N_T cm^{-3}). Rewilded vegetated sediments showed the highest N_T densities (0.00068 ± 0.00022 g N_T cm^{-3}), while unvegetated wild sediments had the lowest. Overall, N_T densities were clearly higher in rewilded saltmarshes (p = 0.003) and in vegetated sediments (p < 0.001; Table 2). N_T stocks in the upper 100 cm of sediment ($N_{T\text{-}100cm}$) were higher in rewilded saltmarshes (3.6 ± 1.6 t N_T ha^{-1}) than in wild saltmarshes (1.6 ± 0.6 t N_T ha^{-1}) (Fig. 5b; F = 31.428, p < 0.001, two-way ANOVA). Similarly, $N_{T\text{-}100cm}$ stocks were slightly higher in vegetated sediments than in unvegetated sediments (2.9 vs 2.3 t N_T ha^{-1}), but this effect was not clear (F = 3.577, p = 0.09, two-way ANOVA; Table S3).

3.4. Nutrient storage and sequestration rates during the rewilding process

The difference in sedimentary C_{org} and N_T stored in the upper 20 cm between wild and rewilded saltmarshes reflects the potential effect of rewilding, assuming an average SAR of 0.69 ± 0.38 cm y^{-1} (Díaz-Almela et al., 2019, 2021). Over 20 years, C_{org} stocks tended to be higher in vegetated than in unvegetated sediments, reaching slightly higher values in vegetated rewilded sediments (15.7 ± 5.7 t ha^{-1}) than in vegetated wild sediments (11.8 ± 4.5 t ha^{-1}), but these differences were not clear (F = 4.660, p = 0.063, two-way ANOVA) (Fig. 5c; Table S3). N_T storage in this period was 0.8 ± 0.3 and 1.1 ± 0.4 t ha^{-1} in vegetated wild and vegetated rewilded saltmarsh sediments, respectively (Fig. 5d), showing a similar trend towards higher values in vegetated sediments, although this difference was not statistically clear (F = 4.544, p = 0.066, two-way ANOVA).

Over the 20-year rewilding period, C_{org} burial rates in the wild saltmarsh were two times higher in vegetated sediments than in unvegetated ones, with values of 133.2 ± 34.9 and 52.8 ± 19.0 g C_{org} m^{-2} y^{-1}, respectively (Fig. 6a). The difference was statistically clear (Tukey HSD, p < 0.001). In contrast, in the rewilded saltmarsh, the average C_{org} burial rate was similar 69.0 ± 21.2 g C_{org} m^{-2} y^{-1}), regardless of vegetation. Thus, burial rates in the rewilded saltmarsh were approximately 26% lower than those in the wild saltmarshes since the onset of rewilding. A similar pattern was found for N_T burial rates (Fig. 6b), with values of 6.8 ± 1.9 g N_T m^{-2} y^{-1} in the rewilded saltmarsh, and 5.6 ± 1.6 and 12.4 ± 2 0.5 g N_T m^{-2} y^{-1} in unvegetated and vegetated wild saltmarsh, respectively.

The stoichiometric ratio of C_{org} to N_T burial rates (mol:mol) showed a trend towards a higher relative accumulation of C_{org} with respect to N_T in the wild vegetated saltmarsh (12.4 ± 2.4), compared to the wild unvegetated sediments (10.8 ± 2.4) and both environments in the rewilded saltmarsh (~12 in both vegetated and unvegetated areas).

3.5. Isotopic analysis

Vertical $\delta^{13}C$ profiles of C_{org} were more negative in the rewilded (−14.1 – (−24.3) ‰) than in the wild saltmarsh (−4.1- (−21.3) ‰) for both vegetated and unvegetated sediments (Fig. S8). At the rewilded site, $\delta^{13}C$ values remained stable with depth in vegetated sediments but became more negative in unvegetated sediments, whereas in the wild saltmarsh they became progressively less negative with depth, regardless of vegetation cover.

The bivariate plot of molar sediment C_{org}:N_T ratio with versus $\delta^{13}C$

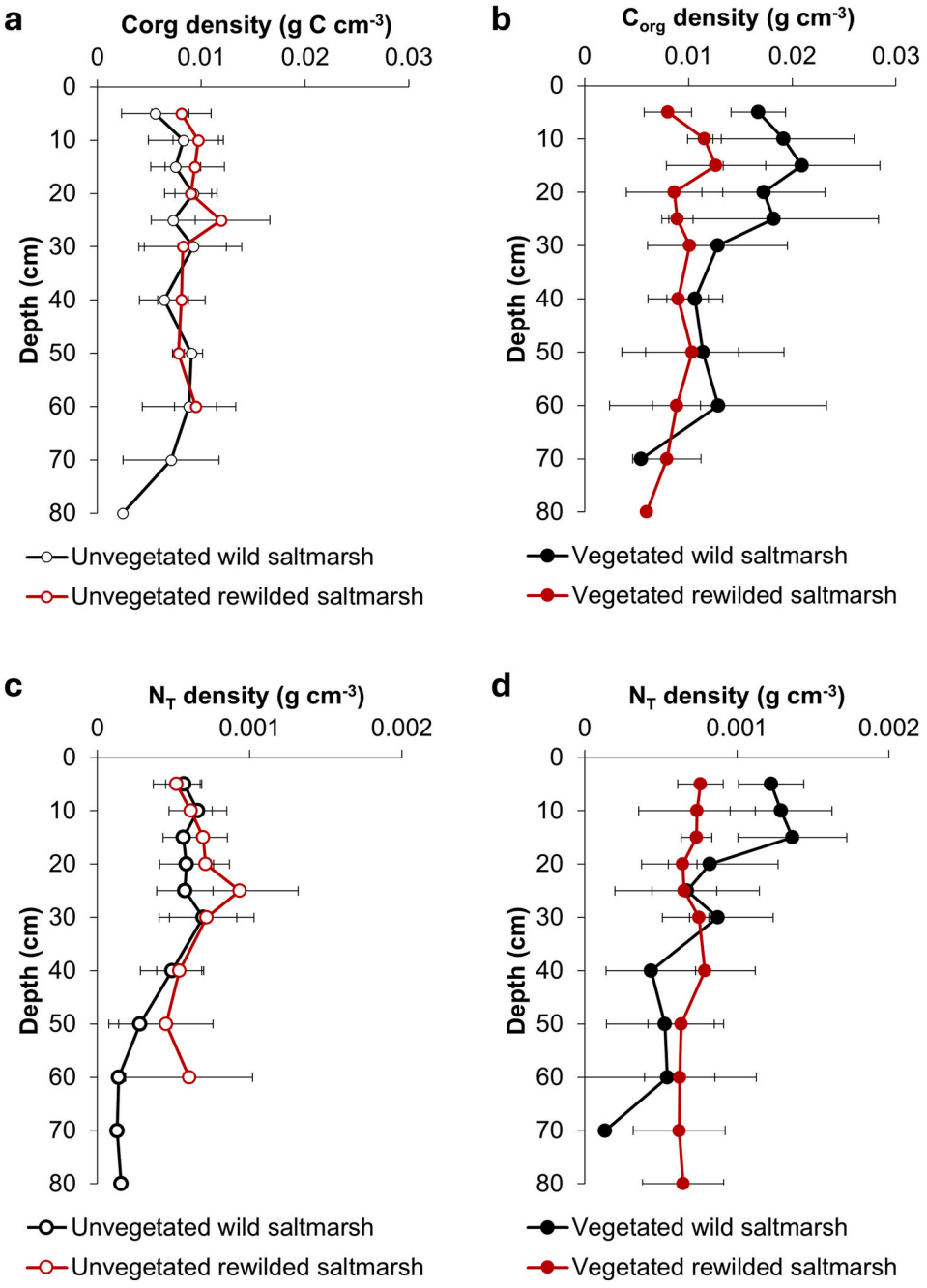

Fig. 4. Vertical profiles of average organic carbon (C_{org}) and total nitrogen (N_T) densities, expressed in g cm^{-3}, in a wild saltmarsh (in black) and in a rewilded saltmarsh (in red) in non-vegetated sediments (a, c) and in vegetated sediments (b, d). Error bars represent the standard deviation (n = 3). The sediment depth was corrected by the compaction factor, and depth intervals were applied. (For interpretation of the references to colour in this figure legend, the reader is referred to the Web version of this article.)

was used to assess differences in OM sources between the two environments and to compare them with potential sources of sedimentary C_{org} (Fig. 7). In the rewilded saltmarsh, the C_{org}:N_T ratio ranged from 13.6 to 20.8 mol C_{org}: mol N_T^{-1} in unvegetated sediment and from 13.3 to 17.2 mol mol^{-1} in vegetated sediments. In comparison, in the wild saltmarsh, the ratio ranged between 8 - 19.1 and 12.9–23.9 mol mol^{-1} for unvegetated and vegetated wild saltmarsh sediments, respectively. This bivariate plot clearly shows what was observed in the $\delta^{13}C$ vertical profiles, i.e., a more negative range of values for the rewilded saltmarshes compared to the wild saltmarshes, particularly for rewilded vegetated sediments, which also presented lower data dispersion. In general, vegetated and unvegetated sediment in rewilded saltmarshes tended to differ more in $\delta^{13}C$ values, while wild vegetated and unvegetated sediment tended to present similar ranges of $\delta^{13}C$, but different ranges of C_{org}:N_T ratios, with higher values in wild vegetated sediment.

The contribution of potential sources to sedimentary C_{org} stored in wild and rewilded saltmarsh sediments was estimated using a Bayesian mixing model. Suspended particulate matter (SPM), Rhodophyta, Chlorophyta, *Caulerpa prolifera*, *Nanozostera noltei*, *Sporobolus maritimus*, and *Sarcocornia* sp. were used in the analysis (Fig. 8), while three other potential sources, i.e. *Halimione portulacoides*, *Cymodocea nodosa*, and Phaeophyceae, were excluded since their isotopic signatures were highly similar to those of *Sarcocornia* sp., *N. noltei* and *S. maritimus*, respectively (Fig. 7). In wild saltmarshes, the macroalga *C. prolifera* was

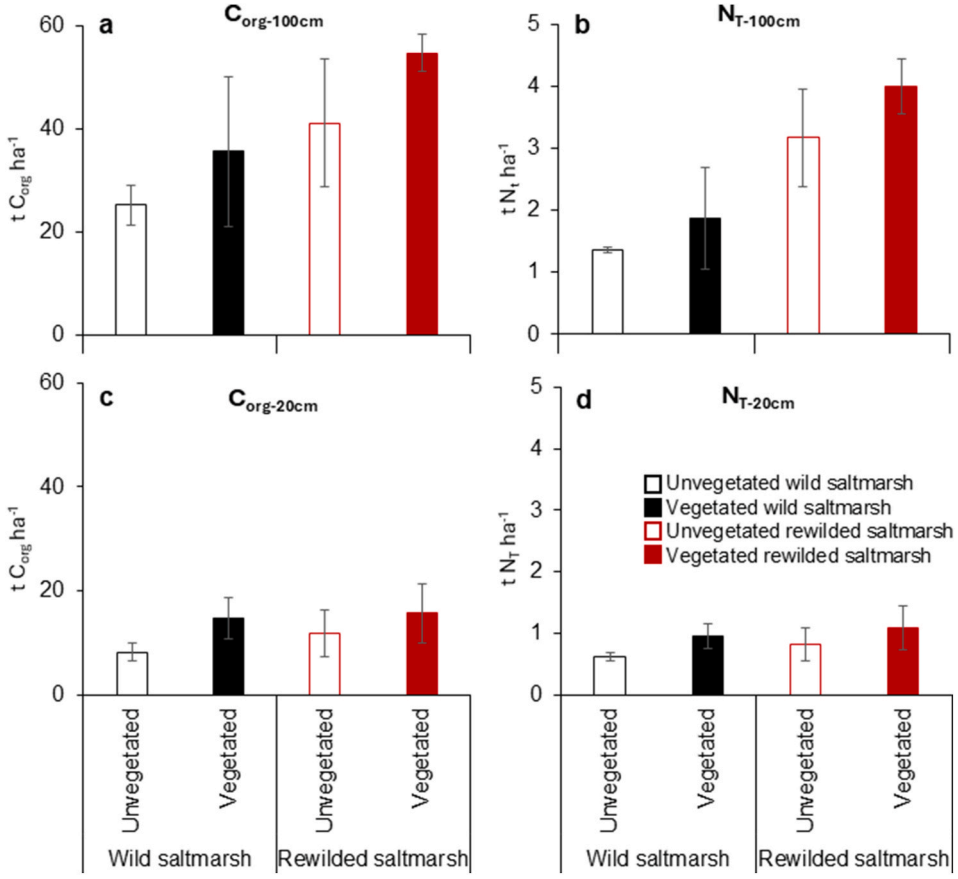

Fig. 5. Stocks of organic carbon (C_{org}) and total nitrogen (N_T) in wild (black) and rewilded (red) saltmarshes, in non-vegetated (empty) and vegetated (filled) sediments: a, b) top 100 cm of sediment (t ha^{-1}); c, d) top 20 cm, representing sediment accumulated during rewilding (2004–2024). Error bars represent the standard deviation (n = 3). (For interpretation of the references to colour in this figure legend, the reader is referred to the Web version of this article.)

the primary contributor, with a median contribution of approximately 40%, followed by SPM (18%), Rhodophyta (10%), Chlorophyta (6%), *N. noltei* (6%), *S. maritimus* (5%), and *Sarcocornia* sp. (4%) (Fig. 8). In contrast, in rewilded saltmarsh sediments, Rhodophyta was the main source, contributing nearly 48%, whereas SPM and *C. prolifera* accounted for approximately 13% and 12%, respectively. The remaining sources, Chlorophyta, *N. noltei*, *S. maritimus*, and *Sarcocornia* sp. contributed between 4% and 9%. Consequently, the contribution of higher saltmarsh vegetation such as *Sporobolus maritimus* and *Sarcocornia* sp. to sedimentary C_{org} storage was surprisingly minimal.

4. Discussion

Rewilding of desiccated saltmarshes reshaped sediment properties and OM distribution, influencing C_{org} and N_T accumulation. Vegetated rewilded sediments accumulated higher OM, whereas wild sediments retained pronounced vertical gradients with elevated C_{org} and N_T in the upper layers. Landsat imagery confirmed vegetation recovery since 2004 following restoration of tidal flow. Despite this recovery, burial rates after 20 years were similar across all areas, emphasizing how sediment characteristics, vegetation, and historical processes interact to determine the long-term storage of C_{org} and N_T. Over the long term, the highest blue carbon stocks were found in vegetated rewilded sediments, regardless of the rewilding process.

4.1. Spatiotemporal changes in saltmarsh vegetation during rewilding

Our findings highlight the capacity of freely available, medium-resolution satellite imagery to monitor the long-term ecological outcomes of coastal rewilding. Using the Landsat series, we show the progressive recovery and eventual stabilization of saltmarsh vegetation following tidal wall reopening, capturing more than two decades of change. Landsat imagery has been widely used to monitor spatiotemporal changes in saltmarsh vegetation (Lopes et al., 2019; Zhang et al., 2023). More recently, other Earth Observation tools have been employed to monitor saltmarshes, including open-source satellite imagery such as Sentinel-2, and drone flights equipped with multi- and hyperspectral cameras or LIDAR detection (Curcio et al., 2023, 2024). However, Landsat imagery remains the only satellite dataset enabling the exploration of spatiotemporal trends dating back to the early 2000s and even earlier. While machine learning or deep learning algorithms can be developed to identify saltmarsh vegetation (Doughty et al., 2024; Naojee et al., 2024), the approach proposed in this study (using NDVI values above 0.25 to differentiate saltmarsh vegetation from bare sediment covered by MPB) has proven effective in detecting saltmarsh vegetation changes over a 30-year period (1994–2024). These NDVI thresholds were based on previous studies conducted in Cadiz Bay on intertidal sediments and saltmarshes, and can be helpful to study long term changes in vegetation cover and quantify the blue carbon storage capacity of these ecosystems (Curcio et al., 2023; Haro et al., 2022).

The increase in vegetation cover and NDVI in the rewilded site, compared with the stability observed in the wild saltmarsh, underscores the capacity of rewilding to drive rapid and sustained recovery of saltmarsh vegetation. Vegetation cover expanded from about 8.9% of the rewilded area (52.4 ha) in 2004, prior to the tidal-wall breaching, to 26.8% (157.9 ha) in 2024, representing an average recovery rate of roughly 1% (5.7 ha) per year. (Fig. 3a; Fig. S2). After the tidal wall was opened in 2004, saltmarsh vegetation first declined between 2004 and

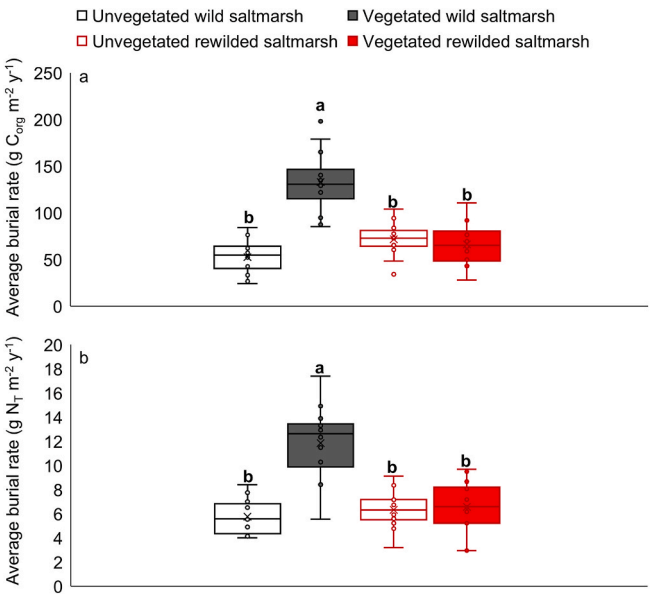

Fig. 6. Box plots of burial rates of organic carbon (C_{org}) and total nitrogen (N_T), expressed as g m^{-2} y^{-1}, within the upper 20 cm of sediment in a wild saltmarsh (in black) and in a rewilded saltmarsh (in red), for non-vegetated (empty bars) and vegetated (filled bars) sediments. The 20 cm depths correspond to vertical accretion accumulated during the rewilding process between 2004 and 2024. The line within each box plot represents the median, and the cross symbol indicates the mean (n = 12). Letters indicate clear differences between groups according to Tukey HSD ($p < 0.05$). (For interpretation of the references to colour in this figure legend, the reader is referred to the Web version of this article.)

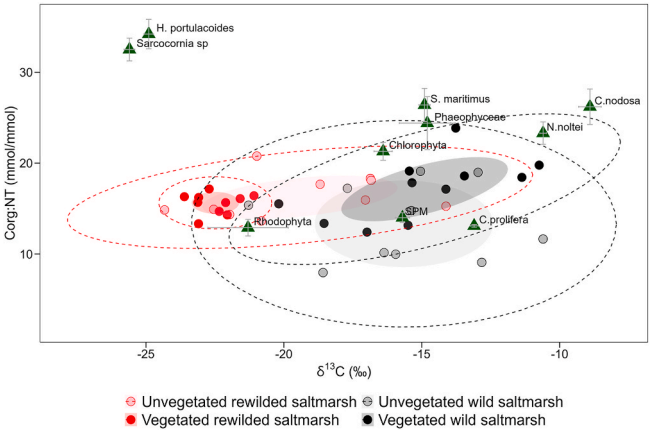

Fig. 7. Bivariate plot of the elemental (C_{org}:N_T) and $\delta^{13}C$ isotopic composition of unvegetated sediments and vegetated sediments from a wild and a rewilded saltmarsh and of some potential sources of organic matter. Shaded ellipses represent the area containing 50% of all values. Dashed line represents the bag expanded by a factor of 3; values outside this region are potential outliers. Potential sources of C_{org} are represented by green triangles, with error bars indicating the standard error. (For interpretation of the references to colour in this figure legend, the reader is referred to the Web version of this article.)

2006, probably because of the sudden change in tidal flooding and the die-off of mid-marsh vegetation near the wall. This early setback, with a loss of between 36 ha y^{-1} in 2006 (Fig. S2), was followed by a faster recovery, above >1.4% y^{-1} from 2008 to 2013, and an oscillating but generally increasing trend up to the present (Fig. 3a). Comparable studies show that our average recovery rate falls within the range reported for other saltmarsh rewilding and recovery studies. Chapple and Dronova (2017) observed vegetation recovery rates of 0.2 ha y^{-1} after a

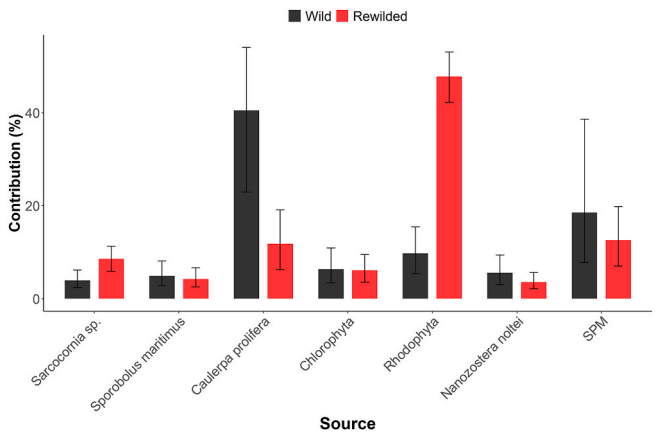

Fig. 8. Estimated contributions of different sources of C_{org} in wild and rewilded saltmarsh sediments estimated with a Bayesian mixing model. Bars represent the median contribution of each source, with error bars indicating the 25th and 75th credibility intervals.

historical drought in California and up to 2.1 ha y^{-1} in wetter years, both notably slower than at our rewilded saltmarsh. van Belzen et al. (2017) reported recovery rates ranging from <0.01 ha y^{-1} in stressed marshes to 0.08–0.13 ha y^{-1} under optimal conditions, indicating that our average rate is moderately high.

Vegetation and bare sediment showed clear oscillations before and after the breach, with recolonization concentrated along the main tidal creek in the north and smaller creeks in the southeast (Fig. 2). While specific ecological factors such as salinity, sedimentation, or elevation that may influence annual recovery rates cannot be fully determined from the available data, the observed patterns provide clear evidence of successful rewilding following historical desiccation and the subsequent re-establishment of tidal exchange. Saltmarsh plants initially recolonized previously desiccated creeks, indicating that natural rewetting during rewilding may facilitate recovery. Despite the 30 m resolution of Landsat imagery and minor tidal variations affecting early detection (Doughty et al., 2024), the analyses captured heterogeneous recolonization patterns. Although recovery rates were modest, they show that a simple passive approach of breaching the tidal wall to restore tidal flow can effectively support long-term restoration. Additional measures, such as creek re-excavation or targeted replanting, could further enhance these gains (Rowland et al., 2024).

NDVI depends on primary producer biomass and their physiological stage and growth, which are assumed to be correlated with chlorophyll content (Gamon et al., 1995; Zhang et al., 2021). In the rewilded saltmarsh, we observed an increase in the average NDVI for bare sediments (from 0.132 to 0.154) and for vegetated saltmarshes (from 0.324 to 0.349) across the entire studied area after the restoration of the tidal flow (Fig. 2; Fig. 3b). These increases were attributed to the recovery of photosynthetic biomass, primarily MPB in the bare sediment environment, and saltmarsh vegetation, mainly *Sporobolus maritimus* and *Sarcocornia* sp. in this area. NDVI values for MPB during the rewilding process were comparable to those reported for temperate tidal flats (Benyoucef et al., 2014; Brito et al., 2013; Van der Wal et al., 2010), including the inner Cadiz Bay (Haro et al., 2022), and for tropical tidal flats (Haro et al., 2025). Similarly, NDVI for the saltmarsh vegetation were in the same range as those reported for *Sarcocornia* spp. and *Sporobolus maritimus*, in saltmarshes located in inner Cadiz Bay (Curcio et al., 2024). While seasonal dynamics of MPB and different species of saltmarsh vegetation have been observed using remote sensing, we decided to exclude the analysis of seasonal dynamics in this long-term study, because the biomass peak of each of the main primary producers in the rewilded saltmarsh occurs in different seasons: MPB in winter, *Sarcocornia* sp. in autumn, and *Sporobolus maritimus* in spring (Curcio et al., 2024; Haro et al., 2022). Therefore, only summer Landsat

images were selected in this study to avoid the biomass peak of the three main primary producers in the area. In this sense, although some overlap in NDVI values between MPB and saltmarsh vegetation may occur, most likely during the recolonization of previously bare sediments by saltmarsh vegetation, the use of summer imagery minimizes this effect, allowing a robust discrimination of saltmarsh vegetation at the spatial and temporal scale considered. Moreover, the use of a conservative NDVI threshold of 0.25 was further verified by visual inspection against RGB composites (Fig. 2), confirming an accurate delineation of saltmarsh vegetation.

4.2. The effect of rewilding on saltmarsh carbon and nitrogen stocks and burial rates

In this study, we attempted to date sediment cores using the ^{210}Pb method; however, the establishment of reliable age-depth models was not possible due to sediment mixing and physical disturbance associated with (1) historical land-use modifications (i.e., saltmarsh desiccation), (2) tidal erosion affecting unvegetated saltmarsh sediments, (3) bioturbation by benthic macrofauna in intertidal sediments or (4) enhanced deposition of fine-grained sediments reported for northern Cadiz Bay since the mid-20th century (Díaz-Almela et al., 2021; Jiménez-Arias et al., 2016; Martínez-Sánchez et al., 2023). Previous studies have documented the highest SAR in the uppermost centimetres of the sediment column in this area (Díaz-Almela et al., 2019). Given these limitations, we assumed a regional SAR_{100y} of 0.69 ± 0.38 cm y^{-1} derived from nearby vegetated, mid-saltmarshes dominated by *Sarcocornia* sp., in the western coastal region of southern Spain (Díaz-Almela et al., 2021). Under these assumptions, the rewilding process that began in 2004 is expected to have affected only the upper ~20 cm of the sediment column (section 2.4).

To assess whether the tidal-wall breaching influenced C_{org} and N_T burial and storage, we compared their stocks in the upper 20 cm ($C_{org\text{-}20cm}$ and $N_{T\text{-}20cm}$) between the rewilded and wild saltmarshes, assuming similar SAR at both saltmarshes. Applying this regional SAR may introduce some bias. The SAR specifically associated with the rewilding period (SAR_{20y}) remains unknown, but is expected to be higher than the long-term average, particularly in the surface layers, as suggested by previously reported SAR profile for Cadiz Bay (Díaz-Almela et al., 2019), together with enhanced deposition of fine-grained sediments reported for northern Cadiz Bay since the mid-20th century (Martínez-Sánchez et al., 2023). Furthermore, the adopted SAR_{100y} value of 0.69 cm y^{-1} falls within the range expected from SAR of 0.5–1 cm y^{-1} reported for Cadiz Bay (assuming sediment accumulation rates of 0.5–1 g sediment cm^{-2} y^{-1} and DBD of 1 g cm^{-3}; Gracia et al., 2017; Jiménez-Arias et al., 2016). Therefore, applying a constant SAR of 0.69 cm y^{-1} and integrating over the upper 20 cm of sediment represents a reasonable and conservative approach for assessing rewilding-induced changes in sedimentary C_{org} and N_T burial. In addition, the vertical profiles of the different variables analysed in this study (Fig. 4, Figs. S4 and S5) showed a change in trend around 20 cm depth in both vegetated and unvegetated sediments of the rewilded saltmarsh. This vertical pattern may indicate a change in the ecological and biogeochemical conditions due to the re-establishment of tides in 2004, supporting the choice of the upper 20 cm of the sediment column to assess rewilding-related changes.

Both $C_{org\text{-}20cm}$ and $N_{T\text{-}20cm}$ stocks were slightly higher in the rewilded saltmarshes compared to the wild ones, although these differences were not statistically clear. This supports the initial hypothesis that rewilded saltmarshes, despite their younger age, can develop C_{org} and N_T storage capacities comparable to than those of reference systems. This finding is consistent with the results reported by Mason et al. (2023), who, after analysing 431 scientific studies worldwide, concluded that restored saltmarshes in Europe stored more C_{org} than natural ones (438.83 ± 191.97 vs 342.1 ± 223.45 t C_{org} ha^{-1}). However, this general trend must be interpreted with caution due to the limited number of European case studies included in the review (n = 22) and the elevated variability observed across reference saltmarshes, within the same region (Díaz-Almela et al., 2019) and globally (Mason et al., 2023). In addition, several studies have shown that the time elapsed since the onset of restoration plays a crucial role in determining sedimentary C_{org} storage (Burden et al., 2019; Call and Bauman, 2021; Gulliver et al., 2020). This highlights the need for further research effort into the potential causes of C_{org} storage variability among saltmarshes. Particularly, studies to analyse the changes in C_{org} stocks along the full trajectory of saltmarsh transformation, from initial natural conditions, through the anthropogenic land use transformation, and during the rewilding or restoration process are essential to fully understand carbon sequestration dynamics in rewilded and restored saltmarshes. However, pre-rewilding C_{org} stocks cannot be measured retrospectively. In this study, although baseline carbon data prior to rewilding are unavailable, the assessment of annual recovery of saltmarsh vegetation using Landsat imagery has provided valuable insights into the pace and trajectory of ecosystem recovery.

Vegetated saltmarshes, both wild and rewilded, tended to store higher C_{org} and N_T than bare sediments in the upper 20 cm (Fig. 5c and d). At the same time, burial rates were consistently highest in vegetated wild saltmarshes, exceeding those in unvegetated wild and both vegetated and unvegetated rewilded sediments over the 20-year rewilding period (Fig. 6). While $C_{org\text{-}20cm}$ and $N_{T\text{-}20cm}$ stocks were higher in vegetated rewilded than in vegetated wild sediments, the average burial rates over the same period showed different results due to the calculation method (section 2.4). Consequently, higher average C_{org} and N_T burial occurred in vegetated wild saltmarshes compared to the rewilded saltmarsh (Fig. 6a) within the upper 20 cm. In the vegetated rewilded saltmarsh, we measured average burial rates of 66 g C_{org} m^{-2} y^{-1} over the first 20 years, which are within the range of values reported for vegetated low-marsh sediments at 100 cm depth in the inner Cadiz Bay (48–91 g C_{org} m^{-2} y^{-1}; de los Santos et al., 2023; Jiménez-Arias et al., 2020).

In the unvegetated rewilded saltmarsh, C_{org} burial averaged 72 g C_{org} m^{-2} y^{-1} during the first 20 years, higher than 53 g C_{org} m^{-2} y^{-1} measured in our unvegetated wild saltmarsh (average for the upper 20 cm) and similar to the 78 g C_{org} m^{-2} y^{-1} reported by Jiménez-Arias et al. (2020) for bare intertidal sediments down to 100 cm depth in the northwestern inner Cadiz Bay. These values are consistent with those reported for temperate saltmarshes in the Eastern England, where C_{org} burial rates reached 104 g C m^{-2} y^{-1} during the first 20 years following managed realignment and declined to 65 g C m^{-2} y^{-1} in later years (Burden et al., 2019). Globally, C burial rates vary widely across regions, with temperate marshes averaging 144 ± 6 g m^{-2} y^{-1} compared with 88.7 ± 3.5 g m^{-2} y^{-1} in the Southern Hemisphere (Wang et al., 2021). The C_{org} burial rates measured in our vegetated wild saltmarsh (averages of 133 g C_{org} m^{-2} y^{-1}), thus, fall within the upper range of values reported for temperate regions as well as globally, which can reach ~250 g C_{org} m^{-2} y^{-1} in reference saltmarsh (Mason et al., 2023). At the ecosystem scale, integrating the mean C_{org} burial rate for vegetated rewilded saltmarshes (66.3 ± 23.8 g C m^{-2} y^{-1}; Fig. 6a) with the observed average annual recovery of vegetated saltmarsh (5.7 ha y^{-1}; Fig. S2) yields a first-order estimate of potential burial of 3.8 ± 1.4 t C_{org} y^{-1} (equivalent to 14 ± 5 t CO_2-eq y^{-1}). Assuming constant rates, this corresponds to a cumulative burial of approximately 76 ± 27 t C_{org} (~277 ± 99 t CO_2-eq) over the 20-year rewilding period. This estimate should be interpreted with caution, as it extrapolates point-based burial rates to the landscape scale and does not account for spatial heterogeneity in SAR and C_{org} burial across the recovering saltmarsh.

Similarly, N_T burial rates in the upper 20 cm of vegetated wild saltmarsh (12 g N_T m^{-2} y^{-1}; Fig. 6b) were higher than those reported for bare intertidal and low-marsh sediments in the inner Cádiz Bay, ranging from ~4 g N_T m^{-2} y^{-1} in the northwestern area (Jiménez-Arias et al., 2020) to 7 g N_T m^{-2} y^{-1} in the southeastern low marshes (de los Santos et al., 2023), and also higher than the 2–5 N_T m^{-2} y^{-1} reported for low-to mid-marsh sediments in the Ria Formosa in Portugal (Martins

et al., 2022). These values are comparable to the ~6 g N_T m^{-2} y^{-1} measured in this study for unvegetated wild and both vegetated and unvegetated rewilded saltmarshes (Table S2), corresponding to 0.4 ± 0.1 t N_T y^{-1} for the vegetated rewilded saltmarsh (i.e., 7.7 ± 2.2 t N_T over the rewilding process). In general, our results support the frequent observation of higher C_{org} stocks and burial rates in vegetated vs. unvegetated sediments, although these differences were not statistically clear in the rewilded saltmarsh. In principle, higher C_{org} and N_T burial rates are expected in vegetated sediments due to enhanced OM accumulation and stabilization (Section B; Supplementary material). However, despite the expansion of saltmarsh vegetation by more than 80% in rewilded areas between 2004 and 2024, this increase has not resulted in a statistically clearly higher C_{org} and N_T sequestration in the accreted sediments. This suggests that the elevated long-term storage of C_{org} and N_T in rewilded saltmarsh is not attributable primarily to the rewilding process, or at least not within a timeframe of just 20 years. Changes in land use from 1958, when the previous saltmarsh was desiccated, up to 2004, when the tidal function was restored, likely had multiple biogeochemical consequences. Expected changes in SAR, sources of OM, dominant pathways and rates of OM diagenetic processes, complicate the interpretation of temporal evolution from available sediment profiles. Overall, our results suggest that, while the capacity of the sediment in the rewilded saltmarsh to store C_{org} and N_T may have largely recovered, two decades may not have been sufficient to allow an important accumulation due to limited sediment deposition (Rowland et al., 2024). These findings contrast with the hypothesis that a rapid recovery of C_{org} and N_T stocks would occur during the initial years following the onset of restoration activities (Call and Bauman, 2021; Gulliver et al., 2020; Mason et al., 2023).

4.3. Blue carbon and nitrogen stocks in saltmarsh sediments

Regardless of the rewilding process, the assessment of C_{org} and N_T stocks down to 1 m depth ($C_{org\text{-}100cm}$ and $N_{T\text{-}100cm}$) across different sedimentary environments, both vegetated and unvegetated, revealed a high degree of variability associated with habitat heterogeneity and vegetation zonation. As expected, $C_{org\text{-}100cm}$ values were consistently slightly higher in vegetated saltmarsh sediments (Fig. 5a, Table S2), a pattern widely reported in the saltmarsh literature, although the magnitude of this difference varied substantially among sites and vegetation types. In this study, sediments vegetated by *Sarcocornia* sp. stored approximately 30–40% more C_{org} than their respective unvegetated sediments, highlighting the role of vegetation and tidal erosion in the net budget of C_{org} sequestration. Overall, sedimentary C_{org} storage ranged between 92.7 and 200.5 t CO_2 ha^{-1} across both wild and rewilded saltmarshes and across vegetated and unvegetated sediments (Table S2). These values fall within the wide range reported for saltmarsh in the region. For instance, similar stocks have been reported for low-marsh *Sporobolus maritimus* in the southeastern inner Cadiz Bay (66.5 t C_{org} ha^{-1}; 243.8 t CO_2 ha^{-1}; de los Santos et al., 2023), for the wild saltmarsh of 'Los Toruños' in Cadiz Bay (232.3–573.2 t CO_2 ha^{-1}; Díaz-Almela et al. (2019)) and in the Odiel saltmarshes (217.6–450.8 t CO_2 ha^{-1}; Díaz-Almela et al. (2019)). In Odiel, a rewetted mid-saltmarsh reported values of up to 609.5 ± 240.4 t CO_2 ha^{-1}, whereas actively restored mid-saltmarsh showed much lower stocks (56.1 ± 34 t CO_2 ha^{-1}; Díaz-Almela et al., 2019). However, C_{org} stocks in the wild and rewilded saltmarshes studied here were within the range of values reported for low-marsh (25–366 t CO_2 ha^{-1}) in Ria Formosa (Martins et al., 2022). This wide variability observed in C_{org} stocks, reflected in both mean values and standard deviations (Table S2), suggests that factors beyond tidal erosion play a key role in controlling long-term C_{org} storage in saltmarsh sediments. These include vegetation zonation (unvegetated sediments dominated by MPB, low-marsh zones dominated by *Sporobolus maritimus*, and mid-marsh zones dominated by *Sarcocornia* sp.), species-specific trapping efficiency, sediment dynamics and the incorporation of predominantly allochthonous OM (Fig. 8).

The $N_{T\text{-}100cm}$ stocks were also slightly higher in vegetated sediments (averages of 1.9 and 4 t N_T ha^{-1}) than in unvegetated ones (average of 1.4 and 3.2 t N_T ha^{-1}) in both saltmarshes. In comparison, somewhat higher stocks have been reported for *Sporobolus maritimus*-dominated low-marsh sediments in the inner Cadiz Bay (5.9 t N_T ha^{-1}; de los Santos et al., 2023) and in the Ria Formosa lagoon (2–10 t N_T ha^{-1}; de los Santos et al., 2019; Martins et al., 2022). As observed in the wild and rewilded saltmarshes in our study, no clear differences in N_T stocks between bare and vegetated sediments have been reported in other systems, such as the South Korean coast, where mean values reached ~6 t N_T ha^{-1} (Kwon et al., 2022) and in the Ria Formosa lagoon (~12 t N_T ha^{-1}; Casal-Porras et al., 2022). Both $C_{org\text{-}100cm}$ and $N_{T\text{-}100cm}$ stocks were clearly higher in rewilded than in wild saltmarshes, although these differences may have existed prior to the rewilding process. The stoichiometric ratio between $C_{org\text{-}100cm}$ and $N_{T\text{-}100cm}$ stocks reflected historical differences in the accumulation of these nutrients. The wild saltmarsh showed an overall C_{org}:N_T ratio of about 22, whereas the rewilded saltmarsh had a ratio of about 15 (Fig. 7). This indicates that the wild saltmarsh stores relatively more C_{org} per unit of N_T, while the rewilded area, despite holding larger absolute amounts of C_{org}, has accumulated proportionally more N_T over time. Such divergences may result from variations in the stoichiometry of OM sources and early diagenetic processes within the sediment. They may also reflect natural spatial heterogeneity in sediment composition along the tidal creek, with sandier deposits near the creek mouth grading landward into finer, muddier sediments, a gradient that becomes strongly accentuated after tidal flow was interrupted by desiccation in the 1960s. Changes in oxygen availability associated with distinct emersion and immersion times, or even with complete penetration of O_2 in desiccated sediment in the rewilded saltmarsh, can alter the mineralization pathways of OM. This may lead to differences in C_{org} content due to stimulation of oxic mineralization. Oxygen availability also affects nitrogen cycling, as it inhibits denitrification and likely promotes the accumulation of N_T in sediments by reducing the release of gaseous nitrogen compounds such as N_2 and N_2O from desiccated sediments (Ji et al., 2015; Peng et al., 2021). Furthermore, N_2O emissions, as a byproduct of nitrification, increase when O_2 concentrations decrease and NO_3^- loads increase. Although the emission of gaseous nitrogen compounds mitigates eutrophication by reducing nitrogen load in coastal environments, N_2O is a potent greenhouse gas and can largely offset the benefits of blue carbon burial. The high complexity of microbial and biogeochemical interactions between C, N, and O_2, combined with the strong spatio-temporal variability of environmental conditions in saltmarshes, makes the interpretation and prediction of nitrogen storage capacity highly challenging at present.

4.4. Potential organic matter sources in rewilded saltmarsh sediment

The differences in $\delta^{13}C$ composition of C_{org} between wild and rewilded saltmarshes suggest notable divergences in the contributions of potential OM sources, a pattern further supported by a Bayesian mixing model applied to pooled vegetated and unvegetated sediments, including the 100 cm layer (Fig. 8). In wild saltmarshes, *Caulerpa prolifera* was the primary contributor to sediment C_{org} (~40%) followed by suspended particulate matter (SPM, 18%) and other estuarine primary producers. The importance of *C. prolifera* as a source of detritus for the sedimentary C_{org} in Cadiz Bay might be due to its extensive coverage (~49%) in the subtidal zone (Haro et al., 2022; Morris et al., 2009), and to the considerable connectivity, via the horizontal transport of SPM, between different habitats within the bay (de los Santos et al., 2023; Jiménez-Arias et al., 2020). Strong tidal mixing and wind-induced turbulence in this shallow coastal ecosystem are likely responsible of the intense exchange of detritus and sediment within the bay (Periáñez et al., 2013; Zarzuelo et al., 2019). In contrast, in the rewilded saltmarsh, Rhodophyta contributed nearly 48% of C_{org}, with similar lower inputs from *C. prolifera* and SPM (~12% each). The dominance of

Rhodophyta as an OM source in the rewilded saltmarsh is unexpected, despite the reported presence of some species, such as *Bostrychia scorpioides* in mid- and low-marsh zones of Cadiz Bay, *Gracilariopsis longissima* in the nearby 'Los Toruños' saltmarsh (Pérez-Lloréns et al., 2004), and other Rhodophyta species across Cadiz Bay (Hernández et al., 2010). The contrasting OM source profiles between wild and rewilded saltmarshes likely reflect differences in hydrodynamic conditions, vegetation cover, connectivity, and OM deposition pathways. Surprisingly, the contribution of higher saltmarsh vegetation, like *Sarcocornia* sp. and *Sporobolus maritimus,* was scarce in both saltmarshes (<8%). This is an unexpected result, as saltmarsh higher plants are generally known to contribute considerably to blue carbon storage (McLeod et al., 2011). However, their habitat characteristics facilitate the trapping of SPM of allochthonous origin, and the relative contribution of autochthonous and allochthonous C_{org} buried in these habitats is likely dependent on site-specific features such as geomorphology or tidal range (Bouillon et al., 2003; Middelburg et al., 1997). Similarly scarce was the contribution of other relevant primary producers in the Cadiz Bay, such as *Nanozostera noltei* or green macroalgae (i.e., Chlorophyta), while they cover substantial fractions of the intertidal area and accumulate clear standing biomass stocks (Haro et al., 2022).

The exclusion of potential sources such as *Halimione portulacoides*, *Cymodocea nodosa*, and *Phaeophyceae* from the model due to isotopic overlap (Fig. 7) highlights a common limitation in source resolution when using stable isotopes (Phillips et al., 2014). A further limitation of this study is the omission of MPB, the main benthic primary producer in the intertidal zones of the inner Cadiz Bay (Haro et al., 2020), whose isotopic signal has never been measured in this mudflat. The isotopic signal of MPB may range between $\delta^{13}C$ values of −23 to −16 ‰; however, this remains poorly constrained (Herman et al., 2000; Middelburg et al., 2000). For this reason, MPB was not included in the Bayesian mixing model, despite its well-documented role as an important source of C_{org} in intertidal sediments (Martins et al., 2022; Middelburg et al., 2000). The apparent contribution of Rhodophyta in the rewilded saltmarsh might also result from overlap with MPB or other uncharacterized sources. Furthermore, our model was limited to a single tracer, combining $\delta^{13}C$ and C_{org}:N_T ratios, since $\delta^{15}N$ was not analysed. Nevertheless, assessing the contribution of potential OM sources to the C_{org} stock down to 100 cm depth is in itself an interesting outcome, as this is rarely addressed, regardless of the rewilding process. Finally, the differences in source profiles between wild and rewilded saltmarshes underscore the variability in potential OM sources across sedimentary habitats within the same ecosystem. In particular, the lower contributions of *C. prolifera* and SPM in rewilded sediments may reflect reduced connectivity with subtidal areas, less efficient trapping of particulate material, or differences in sediment compaction and retention. These characteristics are site-specific and spatially heterogeneous, even within a single saltmarsh, and can influence its long-term carbon sequestration capacity (Ouyang and Lee, 2014).

5. Conclusion

The re-establishment of tidal exchange as a nature-based solution to restore anthropogenically desiccated wetlands plays a pivotal role in promoting saltmarsh vegetation recovery and reinstating ecosystem services related to climate regulation and nutrient cycling. In this study, the rewilded saltmarsh achieved C_{org} and N_T storage capacities (i.e., stocks at 20 cm) that were comparable to those of reference saltmarshes, although evidence for rapid nutrient accumulation during the early years of rewilding is not clearly observed. The highest nutrient stocks were recorded in rewilded saltmarsh, mainly vegetated sediments, indicating that long-term nutrient accumulation was influenced by processes occurring prior to rewilding. These discrepancies raise important questions, such as how many years are required for rewilded saltmarshes to fully restore their ecosystem services and which environmental drivers influence the pace and outcome of the rewilding process.

To evaluate the effects of rewilding and restoration programs on various ecosystem functions, long-term, integrated studies that combine multiple approaches, including direct on-site metabolic measurements using benthic chambers and remote sensing techniques, are essential. Furthermore, increasing the number of long sediment cores analysed for C and N contents and isotopic signatures, despite the high costs involved, is crucial to account for the considerable spatial heterogeneity and complexity of saltmarshes. Future studies should also consider the role of bioturbators, as their sediment reworking may significantly influence carbon and nitrogen distribution and overall ecosystem functioning.

Despite limitations in assessing pre-rewilding sediment conditions and chronological reconstruction, likely caused by sediment mixing in the upper layers produced during land-use transformation, our findings highlight the potential of rewilding to restore key biogeochemical functions and contribute to climate change mitigation and improved nutrient regulation in coastal areas.

CRediT authorship contribution statement

S. Haro: Writing – original draft, Visualization, Methodology, Investigation, Funding acquisition, Formal analysis, Conceptualization. **A. Corzo:** Writing – original draft, Funding acquisition, Conceptualization. **S. Papaspyrou:** Writing – review & editing, Funding acquisition, Conceptualization. **E. García-Robledo:** Writing – review & editing, Conceptualization. **I. Caballero:** Writing – review & editing, Conceptualization. **G.M. Arroyo:** Writing – review & editing, Methodology, Investigation, Funding acquisition, Conceptualization.

Funding

This study was funded by the CEIMAR Foundation through a project for young researchers (CEIJ-005, 2020), AQUA&AMBI (0750_AQUA-&AMBI_2_5_P) funded by Interreg Spain–Portugal, RICAS (TED2021-132439B-I00) funded by MICIU/AEI/10.13039/501100011033 and by the European Union NextGenerationEU/PRTR, and the REWRITE project (101081357 H2020/HORIZON-CL5-2022-D1-02-05) funded by the European Union. Views and opinions expressed are however those of the author(s) only and do not necessarily reflect those of the European Union. Neither the European Union nor the granting authority can be held responsible for them. SH was funded by a regional postdoctoral fellowship (grant DGP_POST_2024_00524), supported by the Junta de Andalucía / CUII and the European Social Fund Plus (FSE+).

Declaration of competing interest

The authors declare that they have no known competing financial interests or personal relationships that could have appeared to influence the work reported in this paper.

Acknowledgments

We thank NASA and the USGS for providing Landsat imagery, and Kady Ramjattan for laboratory sample processing during her Erasmus Mundus internship in the MSc Water and Coastal Management programme.

Appendix A. Supplementary data

Supplementary data to this article can be found online at https://doi.org/10.1016/j.marenvres.2026.107897.

Data availability

Data will be made available on request.

References

Adams, J.B., Raw, J.L., Riddin, T., Wasserman, J., Van Niekerk, L., 2021. Salt marsh restoration for the provision of multiple ecosystem services. Diversity 13, 680. https://doi.org/10.3390/d13120680.

Barbier, E.B., Hacker, S.D., Kennedy, C., Koch, E.W., Stier, A.C., Silliman, B.R., 2011. The value of estuarine and coastal ecosystem services. Ecol. Monogr. 81 (1), 169–193. https://doi.org/10.1890/10-1510.

Barry, A., Ooi, S.K., Helton, A.M., Steven, B., Elphick, C.S., Lawrence, B.A., 2022. Vegetation zonation predicts soil carbon mineralization and microbial communities in southern new England salt marshes. Estuaries Coasts 45, 168–180. https://doi.org/10.1007/s12237-021-00943-0.

Bates, D., Mächler, M., Bolker, B., Walker, S., 2015. Fitting linear mixed-effects models using lme4. J. Stat. Softw. 67. https://doi.org/10.18637/jss.v067.i01.

Beers, L.S., Crooks, S., Fennessy, S., 2020. Desktop study of blue carbon ecosystems in ramsar sites. Report by Silvestrum Climate Associates for the Scientific and Technical Review Panel of the Convention on Wetlands. https://doi.org/10.13140/RG.2.2.17891.22565.

Benyoucef, I., Blandin, E., Lerouxel, A., Jesus, B., Rosa, P., Méléder, V., Launeau, P., Barillé, L., 2014. Microphytobenthos interannual variations in a north-European estuary (Loire estuary, France) detected by visible-infrared multispectral remote sensing. Estuar. Coast Shelf Sci. 136, 43–52. https://doi.org/10.1016/j.ecss.2013.11.007.

Bouillon, S., Dahdouh-Guebas, F., Rao, A.V.V.S., Koedam, N., Dehairs, F., 2003. Sources of organic carbon in mangrove sediments: variability and possible ecological implications. Hydrobiologia 495, 33–39. https://doi.org/10.1023/A:1025411506526.

Brito, A.C., Benyoucef, I., Jesus, B., Brotas, V., Gernez, P., Mendes, C.R., Launeau, P., Dias, M.P., Barillé, L., 2013. Seasonality of microphytobenthos revealed by remote-sensing in a South European estuary. Cont. Shelf Res. 66, 83–91. https://doi.org/10.1016/j.csr.2013.07.004.

Burden, A., Garbutt, A., Evans, C.D., 2019. Effect of restoration on saltmarsh carbon accumulation in Eastern England. Biol. Lett. 15, 3. https://doi.org/10.1098/rsbl.2018.0773.

Burden, A., Garbutt, R.A., Evans, C.D., Jones, D.L., Cooper, D.M., 2013. Carbon sequestration and biogeochemical cycling in a saltmarsh subject to coastal managed realignment. Estuar. Coast Shelf Sci. 120, 12–20. https://doi.org/10.1016/j.ecss.2013.01.014.

Call, S.M., Bauman, J.M., 2021. Tidal marsh plant community development within four restored lowland estuaries in the Western Peninsulas of Washington State, USA. Am. J. Plant Sci. 12, 1543–1558. https://doi.org/10.4236/ajps.2021.1210109.

Casal-Porras, I., de los Santos, C.B., Martins, M., Santos, R., Pérez-Lloréns, J.L., Brun, F.G., 2022. Sedimentary organic carbon and nitrogen stocks of intertidal seagrass meadows in a dynamic and impacted wetland: effects of coastal infrastructure constructions and meadow establishment time. J. Environ. Manag. 322. https://doi.org/10.1016/j.jenvman.2022.115841.

Chapple, D., Dronova, I., 2017. Vegetation development in a tidal marsh restoration project during a historic drought: a remote sensing approach. Front. Mar. Sci. 4. https://doi.org/10.3389/fmars.2017.00243.

Curcio, A.C., Barbero, L., Peralta, G., 2024. Enhancing salt marshes monitoring: estimating biomass with drone-derived habitat-specific models. Remote Sens. Appl. Soc. Environ. 35, 101216. https://doi.org/10.1016/j.rsase.2024.101216.

Curcio, A.C., Barbero, L., Peralta, G., 2023. UAV-hyperspectral imaging to estimate species distribution in salt marshes: a case study in the Cadiz Bay (SW Spain). Remote Sens. 15, 1419. https://doi.org/10.3390/rs15051419.

de Lomas, J.G., García, C.M., Esteban, O.A., 2008. Identificación de Hábitat de interés comunitario y estimaciones preliminares de posibles efectos de su inundación. Rev. la Soc. Gaditana Hist. Nat 5, 9–37.

de los Santos, C.B., Egea, L.G., Martins, M., Santos, R., Masqué, P., Peralta, G., Brun, F.G., Jiménez-Ramos, R., 2023. Sedimentary organic carbon and nitrogen sequestration across a vertical gradient on a temperate wetland seascape including salt marshes, seagrass meadows and rhizophytic macroalgae beds. Ecosystems 26, 826–842. https://doi.org/10.1007/s10021-022-00801-5.

de los Santos, C.B., Krause-Jensen, D., Alcoverro, T., Marbà, N., Duarte, C.M., van Katwijk, M.M., Pérez, M., Romero, J., Sánchez-Lizaso, J.L., Roca, G., Jankowska, E., Pérez-Lloréns, J.L., Fournier, J., Montefalcone, M., Pergent, G., Ruiz, J.M., Cabaço, S., Cook, K., Wilkes, R.J., Moy, F.E., Trayter, G.M.-R., Arañó, X.S., de Jong, D.J., Fernández-Torquemada, Y., Auby, I., Vergara, J.J., Santos, R., 2019. Recent trend reversal for declining European seagrass meadows. Nat. Commun. 10, 3356. https://doi.org/10.1038/s41467-019-11340-4.

Díaz-Almela, E., Piñeiro-Juncal, N., Marco-Méndez, C., Giralt, S., Leiva-Dueñas, C., Mateo, M.A., 2019. Carbon Stocks and Fluxes Associated to Andalusian Saltmarshes. Deliverable C2.2, Project LIFE Blue Natura (LIFE14CCM/ES/000957), vol. 2. UICN, p. 84.

Díaz-Almela, E., Piñeiro-juncal, N., Soler, M., Marco-Méndez, C., Belshe, E.F., Leiva-Dueñas, C., Lavery, P.S., Giralt, S., Mateo, M.Á., 2021. Las marismas de marea andaluzas como sumidero y almacén de carbono orgánico. Chron. naturae 8, 35–56.

Doughty, C.L., Cavanaugh, K.C., Chapman, S., Fatoyinbo, L., 2024. Uncovering mangrove range limits using very high resolution satellite imagery to detect fine-scale mangrove and saltmarsh habitats in dynamic coastal ecotones. Remote Sens. Ecol. Conserv 686–701. https://doi.org/10.1002/rse2.394.

Duarte, C.M., Middelburg, J.J., Caraco, N., 2005. Major role of marine vegetation on the oceanic carbon cycle. Biogeosciences 2, 1–8. https://doi.org/10.5194/bg-2-1-2005.

Dushoff, J., Kain, M.P., Bolker, B.M., 2019. I can see clearly now: reinterpreting statistical significance. Methods Ecol. Evol. 10, 756–759. https://doi.org/10.1111/2041-210X.13159.

Fox, J., Weisberg, S., 2011. An R Companion to Applied Regression, 3rd. ed. Sage, Thousand Oaks, CA.

Gamon, J.A., Field, C.B., Goulden, M.L., Griffin, K.L., Hartley, A.E., Joel, G., Penuelas, J., Valentini, R., 1995. Relationships between NDVI, canopy structure, and photosynthesis in three californian vegetation types. Ecol. Appl. 5, 28–41. https://doi.org/10.2307/1942049.

Gann, G.D., McDonald, T., Walder, B., Aronson, J., Nelson, C.R., Jonson, J., Hallett, J.G., Eisenberg, C., Guariguata, M.R., Liu, J., Hua, F., Echeverría, C., Gonzales, E., Shaw, N., Decleer, K., Dixon, K.W., 2019. International principles and standards for the practice of ecological restoration. Restor. Ecol. 27, S1–S46. https://doi.org/10.1111/rec.13035. Second edition.

Gonçalves, C., Fernandes, J., Neto, J.M., Veríssimo, H., Caçador, I., Verdelhos, T., 2024. Evolution and effectiveness of Salt Marsh restoration: a bibliometric analysis. Water 16, 1175. https://doi.org/10.3390/w16081175.

González, C.J., Torres, J.R., Haro, S., Gómez-Enri, J., Álvarez, Ó., 2023. High-resolution characterization of intertidal areas and lowest astronomical tidal surface by use of Sentinel-2 multispectral imagery and hydrodynamic modeling: Case-study in Cadiz Bay (Spain). Sci. Total Environ. 861, 160620. https://doi.org/10.1016/j.scitotenv.2022.160620.

Gore, C., Gehrels, W.R., Smeaton, C., Andrews, L., McMahon, L., Hibbert, F., Austin, W.E.N., Nolte, S., Garrett, E., 2024. Saltmarsh blue carbon accumulation rates and their relationship with sea-level rise on a multi-decadal timescale in northern England. Estuar. Coast Shelf Sci. 299, 108665. https://doi.org/10.1016/j.ecss.2024.108665.

Gracia, F.J., Alonso Villalobos, C., Abarca, J.M., 2017. Evolución histórica y geomorfología de las explotaciones salineras en marismas mareales. Ejemplos de la bahía de Cádiz. Cuaternario Geomorfol. 31, 45–72. https://doi.org/10.17735/cyg.v31i1-2.54681.

Graves, S., Hans-Peter, P., Selzer, L., 2012. Multcompview: Visualizations of Paired ComparisonsSpencer. CRAN Contrib. Packag. https://doi.org/10.32614/CRAN.package.multcompView.

Gulliver, A., Carnell, P.E., Trevathan-Tackett, S.M., Duarte de Paula Costa, M., Masqué, P., Macreadie, P.I., 2020. Estimating the potential blue carbon gains from tidal marsh rehabilitation: a case study from south Eastern Australia. Front. Mar. Sci. 7, 1–13. https://doi.org/10.3389/fmars.2020.00403.

Haro, S., Jesus, B., Oiry, S., Papaspyrou, S., Lara, M., González, C.J., Corzo, A., 2022. Microphytobenthos spatio-temporal dynamics across an intertidal gradient using Random Forest classification and Sentinel-2 imagery. Sci. Total Environ. 804, 149983. https://doi.org/10.1016/j.scitotenv.2021.149983.

Haro, S., Lara, M., Laiz, I., González, C.J., Bohórquez, J., Garcia-Robledo, E., Corzo, A., Papaspyrou, S., 2020. Microbenthic net metabolism along intertidal gradients (Cadiz Bay, SW Spain): Spatio-Temporal patterns and environmental factors. Front. Mar. Sci. 7. https://doi.org/10.3389/fmars.2020.00039.

Haro, S., Mucheye, T., Caballero, I., Priego, B., Gonzalez, C.J., Gómez-Ramírez, E.H., Corzo, A., Papaspyrou, S., 2025. Microphytobenthos spatio-temporal dynamics across an intertidal gradient in a tropical Estuary using Sentinel-2 imagery. Sci. Total Environ. 963, 178516. https://doi.org/10.1016/j.scitotenv.2025.178516.

Heiri, O., Lotter, A.F., Lemcke, G., 2001. Loss on ignition as a method for estimating organic and carbonate content in sediments: reproducibility and comparability of results. J. Paleolimnol. 25, 101–110.

Herman, P., Middelburg, J., Widdows, J., Lucas, C., Heip, C., 2000. Stable isotopes as trophic tracers: combining field sampling and manipulative labelling of food resources for macrobenthos. Mar. Ecol. Prog. Ser. 204, 79–92. https://doi.org/10.3354/meps204079.

Hernández, I., Bermejo, R., Pérez-Lloréns, J.L., Vergara, J.J., 2010. Contribución al conocimiento de los macrófitos marinos del saco interno y caños adyacentes de la bahía de Cádiz. Soc. Española Ficología 43, 11–16.

Hothorn, T., Bretz, F., Westfall, P., 2008. Simultaneous inference in general parametric models. Biom. J. 50, 346–363. https://doi.org/10.1002/bimj.200810425.

Howard, J., Hoyt, S., Isensee, K., Pidgeon, E., Telszewski, M., 2014. Coastal Blue Carbon: Methods for Assessing Carbon Stocks and Emissions Factors in Mangroves, Tidal Salt Marshes, and Seagrass Meadows. Conserv. Int. Intergov. Oceanogr. Comm. UNESCO, Int. Union Conserv. Nature. Arlington, Virginia, USA.

Howard, J., Sutton-Grier, A., Herr, D., Kleypas, J., Landis, E., Mcleod, E., Pidgeon, E., Simpson, S., 2017. Clarifying the role of coastal and marine systems in climate mitigation. Front. Ecol. Environ. 15, 42–50. https://doi.org/10.1002/fee.1451.

Ji, Q., Babbin, A.R., Peng, X., Bowen, J.L., Ward, B.B., 2015. Nitrogen substrate–dependent nitrous oxide cycling in salt marsh sediments. J. Mar. Res. 73, 71–92. https://doi.org/10.1357/002224015815848820.

Jiménez-Arias, J.L., Mata, M.P., Corzo, A., Poulton, S.W., März, C., Sánchez-Bellón, A., Martínez-López, J., Casas-Ruiz, M., Garcia-Robledo, E., Bohórquez, J., Papaspyrou, S., 2016. A multiproxy study distinguishes environmental change from diagenetic alteration in the recent sedimentary record of the inner Cadiz Bay (SW Spain). Holocene 26, 1355–1370. https://doi.org/10.1177/0959683616640046.

Jiménez-Arias, J.L., Morris, E.P., Rubio-de-Inglés, M.J., Peralta, G., Garcia-Robledo, E., Corzo, A., Papaspyrou, S., 2020. Tidal elevation is the key factor modulating burial rates and composition of organic matter in a coastal wetland with multiple habitats. Sci. Total Environ. 724, 138205. https://doi.org/10.1016/j.scitotenv.2020.138205.

Komada, T., Anderson, M.R., Dorfmeier, C.L., 2008. Carbonate removal from coastal sediments for the determination of organic carbon and its isotopic signatures, δ 13 C and Δ 14 C: comparison of fumigation and direct acidification by hydrochloric acid. Limnol Oceanogr. Methods 6, 254–262. https://doi.org/10.4319/lom.2008.6.254.

Kwon, I., Lee, C., Lee, Jongmin, Kim, B., Park, S.Y., Kim, J., Lee, Junghyun, Noh, J., Kwon, B.-O., Son, S., Yoon, H.J., Nam, J., Choi, K., Khim, J.S., 2022. The first national scale evaluation of total nitrogen stocks and burial rates of intertidal sediments along the entire coast of South Korea. Sci. Total Environ., 154320 https://doi.org/10.1016/j.scitotenv.2022.154320.

Lenth, R., Piaskowski, J., 2025. Emmeans: Estimated Marginal Means, Aka Least-Squares Means (Versión 2.0.0).
Lopes, C.L., Mendes, R., Caçador, I., Dias, J.M., 2019. Evaluation of long-term estuarine vegetation changes through Landsat imagery. Sci. Total Environ. 653, 512–522. https://doi.org/10.1016/j.scitotenv.2018.10.381.
Lotze, H.K., Lenihan, H.S., Bourque, B.J., Bradbury, R.H., Cooke, R.G., Kay, M.C., Kidwell, S.M., Kirby, M.X., Peterson, C.H., Jackson, J.B.C., 2006. Depletion, degradation, and recovery potential of estuaries and coastal seas. Science 312, 1806–1809. https://doi.org/10.1126/science.1128035 (80).
Macreadie, P.I., Anton, A., Raven, J.A., Beaumont, N., Connolly, R.M., Friess, D.A., Kelleway, J.J., Kennedy, H., Kuwae, T., Lavery, P.S., Lovelock, C.E., Smale, D.A., Apostolaki, E.T., Atwood, T.B., Baldock, J., Bianchi, T.S., Chmura, G.L., Eyre, B.D., Fourqurean, J.W., Hall-Spencer, J.M., Huxham, M., Hendriks, I.E., Krause-Jensen, D., Laffoley, D., Luisetti, T., Marbà, N., Masque, P., McGlathery, K.J., Megonigal, J.P., Murdiyarso, D., Russell, B.D., Santos, R., Serrano, O., Silliman, B.R., Watanabe, K., Duarte, C.M., 2019. The future of Blue Carbon science. Nat. Commun. 10, 3998. https://doi.org/10.1038/s41467-019-11693-w.
Martin, C.L., Momtaz, S., Gaston, T., Moltschaniwskyj, N.A., 2020. Estuarine cultural ecosystem services valued by local people in New South Wales, Australia, and attributes important for continued supply. Ocean Coast Manag. 190, 105160. https://doi.org/10.1016/j.ocecoaman.2020.105160.
Martínez-Sánchez, A., Gracia, F.J., Alonso, C., Mata, E., Caporizzo, C., 2023. Reconstructing the historical shoreline evolution of the Northern Bay of Cádiz (SW Spain) from geomorphological and geoarchaeological data. J. Maps 19. https://doi.org/10.1080/17445647.2023.2206585.
Martins, M., de los Santos, C.B., Masqué, P., Carrasco, A.R., Veiga-Pires, C., Santos, R., 2022. Carbon and nitrogen stocks and burial rates in intertidal vegetated habitats of a mesotidal coastal lagoon. Ecosystems 25, 372–386. https://doi.org/10.1007/s10021-021-00660-6.
Mason, V.G., Burden, A., Epstein, G., Jupe, L.L., Wood, K.A., Skov, M.W., 2023. Blue carbon benefits from global saltmarsh restoration. Glob. Change Biol. 29, 6517–6545. https://doi.org/10.1111/gcb.16943.
McDonald, T., Gann, G.D., Jonson, J., Dixon, K.W., Aronson, J., Decleer, K., Hallett, J., Keenleyside, K., Nelson, C., Walder, B., Wickwire, L., 2016. International standards for the practice of ecological restoration – including principles and key concepts. Rapport Niet Door INBO Uitgegeven BT - International Standards for the Practice of Ecological Restoration – including Principles and Key Concepts.
McLeod, E., Chmura, G.L., Bouillon, S., Salm, R., Björk, M., Duarte, C.M., Lovelock, C.E., Schlesinger, W.H., Silliman, B.R., 2011. A blueprint for blue carbon: toward an improved understanding of the role of vegetated coastal habitats in sequestering CO2. Front. Ecol. Environ. 9, 552–560. https://doi.org/10.1890/110004.
Mei, W., Dong, H., Gao, X., Liu, H., Qian, L., Fu, X., Wang, L., 2025. Response of key nitrogen removal processes in estuarine salt marshes to different plant harvesting patterns varies significantly across different time scales. J. Environ. Manag. 377, 124544. https://doi.org/10.1016/j.jenvman.2025.124544.
Middelburg, J.J., Barranguet, C., Boschker, H.T.S., Herman, P.M.J., Moens, T., Heip, C.H. R., 2000. The fate of intertidal microphytobenthos carbon: an in situ 13 c-labeling study. Limnol. Oceanogr. 45, 1224–1234. https://doi.org/10.4319/lo.2000.45.6.1224.
Middelburg, J.J., Nieuwenhuize, J., Lubberts, R.K., Van De Plassche, O., 1997. Organic carbon isotope systematics of coastal marshes. Estuar. Coast Shelf Sci. 45, 681–687. https://doi.org/10.1006/ecss.1997.0247.
Morris, E.P., Peralta, G., Benavente, J., Freitas, R., Rodrigues, A.M., Quintino, V., Alvarez, O., Valcárcel-pérez, N., 2009. Caulerpa prolifera stable isotope ratios reveal anthropogenic nutrients within a tidal lagoon. Mar. Ecol. Prog. Ser. 390, 117–128. https://doi.org/10.3354/meps08184.
Moseman-Valtierra, S., Gonzalez, R., Kroeger, K.D., Tang, J., Chao, W.C., Crusius, J., Bratton, J., Green, A., Shelton, J., 2011. Short-term nitrogen additions can shift a coastal wetland from a sink to a source of N2O. Atmos. Environ. 45, 4390–4397. https://doi.org/10.1016/j.atmosenv.2011.05.046.
Murray, N.J., Phinn, S.R., DeWitt, M., Ferrari, R., Johnston, R., Lyons, M.B., Clinton, N., Thau, D., Fuller, R.A., 2019. The global distribution and trajectory of tidal flats. Nature 565, 222–225. https://doi.org/10.1038/s41586-018-0805-8.
Naojee, S.M., LaRocque, A., Leblon, B., Norris, G.S., Barbeau, M.A., Rowland, M., 2024. Monitoring saltmarsh restoration in the upper Bay of Fundy using multi-temporal Sentinel-2 imagery and random forests classifier. Remote Sens. 16, 4667. https://doi.org/10.3390/rs16244667.
Ouyang, X., Lee, S.Y., 2014. Updated estimates of carbon accumulation rates in coastal marsh sediments. Biogeosciences 11, 5057–5071. https://doi.org/10.5194/bg-11-5057-2014.
Parnell, A.C., Phillips, D.L., Bearhop, S., Semmens, B.X., Ward, E.J., Moore, J.W., Jackson, A.L., Grey, J., Kelly, D.J., Inger, R., 2013. Bayesian stable isotope mixing models. Environmetrics 24, 387–399. https://doi.org/10.1002/env.2221.
Pedersen, T.L., 2016. Ggforce: Accelerating “Ggplot2.”. CRAN Contrib. Packag. https://doi.org/10.32614/CRAN.package.ggforce.
Pendleton, L., Donato, D.C., Murray, B.C., Crooks, S., Jenkins, W.A., Sifleet, S., Craft, C., Fourqurean, J.W., Kauffman, J.B., Marbà, N., Megonigal, P., Pidgeon, E., Herr, D., Gordon, D., Baldera, A., 2012. Estimating global “Blue Carbon” emissions from conversion and degradation of vegetated coastal ecosystems. PLoS One 7. https://doi.org/10.1371/journal.pone.0043542.
Peng, X., Ji, Q., Angell, J.H., Kearns, P.J., Bowen, J.L., Ward, B.B., 2021. Long-Term fertilization alters nitrous oxide cycling dynamics in Salt Marsh sediments. Environ. Sci. Technol. 55, 10832–10842. https://doi.org/10.1021/acs.est.1c01542.
Periáñez, R., Casas-Ruíz, M., Bolívar, J.P., 2013. Tidal circulation, sediment and pollutant transport in Cádiz Bay (SW Spain): a modelling study. Ocean. Eng. 69, 60–69. https://doi.org/10.1016/j.oceaneng.2013.05.016.
Perino, A., Pereira, H.M., Navarro, L.M., Fernández, N., Bullock, J.M., Ceauşu, S., Cortés-Avizanda, A., Van Klink, R., Kuemmerle, T., Lomba, A., Pe'er, G., Plieninger, T., Benayas, J.M.R., Sandom, C.J., Svenning, J.C., Wheeler, H.C., 2019. Rewilding complex ecosystems. Science 364. https://doi.org/10.1126/science.aav5570 (80).
Pétillon, J., McKinley, E., Alexander, M., Adams, J.B., Angelini, C., Balke, T., Griffin, J. N., Bouma, T., Hacker, S., He, Q., Hensel, M.J.S., Ibáñez, C., Macreadie, P.I., Martino, S., Sharps, E., Ballinger, R., de Battisti, D., Beaumont, N., Burdon, D., Daleo, P., D'Alpaos, A., Duggan-Edwards, M., Garbutt, A., Jenkins, S., Ladd, C.J.T., Lewis, H., Mariotti, G., McDermott, O., Mills, R., Möller, I., Nolte, S., Pagès, J.F., Silliman, B., Zhang, L., Skov, M.W., 2023. Top ten priorities for global saltmarsh restoration, conservation and ecosystem service research. Sci. Total Environ. 898. https://doi.org/10.1016/j.scitotenv.2023.165544.
Pettorelli, N., Bullock, J.M., 2023. Restore or rewild? Implementing complementary approaches to bend the curve on biodiversity loss. Ecol. Solut. Evid. 4, 1–7. https://doi.org/10.1002/2688-8319.12244.
Phillips, D.L., Inger, R., Bearhop, S., Jackson, A.L., Moore, J.W., Parnell, A.C., Semmens, B.X., Ward, E.J., 2014. Best practices for use of stable isotope mixing models in food-web studies. Can. J. Zool. 92, 823–835. https://doi.org/10.1139/cjz-2014-0127.
Rowland, P.I., Wartman, M., Bursic, J., Carnell, P., 2024. Restored and created tidal marshes recover ecosystem services over time. Environ. Sustain. Indic. 24, 100539. https://doi.org/10.1016/j.indic.2024.100539.
Saintilan, N., Kovalenko, K.E., Guntenspergen, G., Rogers, K., Lynch, J.C., Cahoon, D.R., Lovelock, C.E., Friess, D.A., Ashe, E., Krauss, K.W., Cormier, N., Spencer, T., Adams, J.B., Raw, J., Ibanez, C., Scarton, F., Temmerman, S., Meire, P., Maris, T., Thorne, K., Brazner, J., Chmura, G.L., Bowron, T., Gamage, V.P., Cressman, K., Endris, C., Marconi, C., Marcum, P., St Laurent, K., Reay, W., Raposa, K.B., Garwood, J.A., Khan, N., 2022. Constraints on the adjustment of tidal marshes to accelerating sea level rise. Science 377, 523–527. https://doi.org/10.1126/science.abo7872 (80).
Santos, R., Duque-Núñez, N., de los Santos, C.B., Martins, M., Carrasco, A.R., Veiga-Pires, C., 2019. Superficial sedimentary stocks and sources of carbon and nitrogen in coastal vegetated assemblages along a flow gradient. Sci. Rep. 9, 1–11. https://doi.org/10.1038/s41598-018-37031-6.
Stewart-Sinclair, P.J., Bulmer, R.H., Macpherson, E., Lundquist, C.J., 2024. Enabling coastal blue carbon in Aotearoa New Zealand: opportunities and challenges. Front. Mar. Sci. 11, 1–6. https://doi.org/10.3389/fmars.2024.1290107.
Temmink, R.J.M., Lamers, L.P.M., Angelini, C., Bouma, T.J., Fritz, C., van de Koppel, J., Lexmond, R., Rietkerk, M., Silliman, B.R., Joosten, H., van der Heide, T., 2022. Recovering wetland biogeomorphic feedbacks to restore the world's biotic carbon hotspots. Science 376. https://doi.org/10.1126/science.abn1479 (80).
van Belzen, J., van de Koppel, J., Kirwan, M.L., van der Wal, D., Herman, P.M.J., Dakos, V., Kéfi, S., Scheffer, M., Guntenspergen, G.R., Bouma, T.J., 2017. Vegetation recovery in tidal marshes reveals critical slowing down under increased inundation. Nat. Commun. 8, 15811. https://doi.org/10.1038/ncomms15811.
Van der Wal, D., Wielemaker-van den Dool, A., Herman, P.M.J., 2010. Spatial synchrony in intertidal benthic algal biomass in temperate coastal and estuarine ecosystems. Ecosystems 13, 338–351. https://doi.org/10.1007/s10021-010-9322-9.
Venables, W.N., Ripley, B.D., 2002. Modern applied statistics with S, 2022. In: Statistics and Computing. Springer, New York.
Wang, F., Sanders, C.J., Santos, I.R., Tang, J., Schuerch, M., Kirwan, M.L., Kopp, R.E., Zhu, K., Li, X., Yuan, J., Liu, W., Li, Z., 2021. Global blue carbon accumulation in tidal wetlands increases with climate change. Natl. Sci. Rev. 8. https://doi.org/10.1093/nsr/nwaa296.
Wickham, H., 2016. ggplot2: Elegant Graphics for Data Analysis.
Wickham, H., Bryan, J., 2015. Readxl: Read Excel Files. CRAN Contrib. Packag. https://doi.org/10.32614/CRAN.package.readxl.
Yang, J.-Y.T., Hsu, T.-C., Tan, E., Lee, K., Krom, M.D., Kang, S., Dai, M., Hsiao, S.S.-Y., Yan, X., Zou, W., Tian, L., Kao, S.-J., 2022. Sedimentary processes dominate nitrous oxide production and emission in the hypoxic zone off the Changjiang River estuary. Sci. Total Environ. 827, 154042. https://doi.org/10.1016/j.scitotenv.2022.154042.
Zarzuelo, C., D'Alpaos, A., Carniello, L., López-Ruiz, A., Díez-Minguito, M., Ortega-Sánchez, M., 2019. Natural and human-induced flow and sediment transport within tidal Creek networks influenced by Ocean-Bay tides. Water 11, 1493. https://doi.org/10.3390/w11071493.
Zarzuelo, C., López-Ruiz, A., Bermúdez, M., Ortega-Sánchez, M., 2023. Measurements and modeling of water levels, currents, density, and wave climate on a semi-enclosed tidal bay, Cádiz (southwest Spain). Earth Syst. Sci. Data 15, 3095–3110. https://doi.org/10.5194/essd-15-3095-2023.
Zhang, T., Tian, B., Wang, Y., Liu, D., Sun, S., Duan, Y., Zhou, Y., 2021. Quantifying seasonal variations in microphytobenthos biomass on estuarine tidal flats using Sentinel-1/2 data. Sci. Total Environ. 777, 146051. https://doi.org/10.1016/j.scitotenv.2021.146051.
Zhang, X., Xiao, X., Wang, X., Xu, X., Qiu, S., Pan, L., Ma, J., Ju, R., Wu, J., Li, B., 2023. Continual expansion of Spartina alterniflora in the temperate and subtropical coastal zones of China during 1985–2020. Int. J. Appl. Earth Obs. Geoinf. 117, 103192. https://doi.org/10.1016/j.jag.2023.103192.